AMMRC CTR 76-5

FINISHING TECHNIQUES FOR SILICON NITRIDE BEARINGS

March 1976

H. R. BAUMGARTNER
Norton Company
Worcester, Massachusetts 01606

PAUL E. COWLEY
Federal Mogul Corporation
Ann Arbor, Michigan 48104

Final Report - Contract DAAG46-74-C-0055

Prepared for

ARMY MATERIALS AND MECHANICS RESEARCH CENTER
Watertown, Massachusetts 02172

This project was accomplished as part of the U.S. Army Manufacturing Technology program. The primary objective of this program is to develop, on a timely basis, manufacturing processes, techniques, and equipment for use in production of Army Materiel. This project was funded by the U.S. Army Troop Support Command under Project No. 7745506.

UNCLASSIFIED

SECURITY CLASSIFICATION OF THIS PAGE (When Data Entered)

REPORT DOCUMENTATION PAGE		READ INSTRUCTIONS BEFORE COMPLETING FORM
1. REPORT NUMBER AMMRC CTR 76-5	2. GOVT ACCESSION NO.	3. RECIPIENT'S CATALOG NUMBER
4. TITLE (and Subtitle) FINISHING TECHNIQUES FOR SILICON NITRIDE BEARINGS		5. TYPE OF REPORT & PERIOD COVERED Final Report 15Jan74 - 15Jul75 6. PERFORMING ORG. REPORT NUMBER
7. AUTHOR(s) H. R. Baumgartner, Norton Company, Worcester, MA 01606 Paul E. Cowley, Federal Mogul Corp, Ann Arbor, MI 48104		8. CONTRACT OR GRANT NUMBER(s) DAAG46-74-C-0055
9. PERFORMING ORGANIZATION NAME AND ADDRESS		10. PROGRAM ELEMENT, PROJECT, TASK AREA & WORK UNIT NUMBERS D/A Project: 7745506 AMCMS Code: 5397-07-5506 Agency Accession:
11. CONTROLLING OFFICE NAME AND ADDRESS Army Materials and Mechanics Research Center Watertown, Massachusetts 02172		12. REPORT DATE March 1976 13. NUMBER OF PAGES 71
14. MONITORING AGENCY NAME & ADDRESS(if different from Controlling Office)		15. SECURITY CLASS. (of this report) Unclassified 15a. DECLASSIFICATION/DOWNGRADING SCHEDULE

16. DISTRIBUTION STATEMENT (of this Report)

Approved for public release; distribution unlimited.

17. DISTRIBUTION STATEMENT (of the abstract entered in Block 20, if different from Report)

18. SUPPLEMENTARY NOTES

19. KEY WORDS (Continue on reverse side if necessary and identify by block number)

Silicon nitride
Bearings
Surface finishing
Physical properties
Characterization

20. ABSTRACT (Continue on reverse side if necessary and identify by block number)

Strength, surface finish and rolling contact fatigue life were determined on two grades of hot pressed silicon nitride after a total of twenty-seven different surface finishing procedures. Rolling contact fatigue lives of silicon nitride with selected smoother finishes tested at 800 ksi Hertz stress were an order of magnitude longer than those obtained on the M50 bearing steel controls and more than twice as long as the best results previously obtained on silicon nitride.

DD FORM 1 JAN 73 1473 EDITION OF 1 NOV 65 IS OBSOLETE

UNCLASSIFIED

SECURITY CLASSIFICATION OF THIS PAGE (When Data Entered)

SUMMARY

The optimum finishing techniques required to provide long life to ceramic roller bearings were investigated. Strength, surface finish and rolling contact fatigue life were determined on two grades of hot pressed silicon nitride after a total of twenty-seven different surface finishing procedures. These procedures all started with diamond grinding but involved a variety of final steps including honing, lapping and silicon carbide grinding. Rolling contact fatigue lives of silicon nitride with selected smoother finishes tested at 800 ksi Hertz stress were an order of magnitude longer than those obtained on the M50 bearing steel controls and more than twice as long as the best results previously obtained on silicon nitride. Statistically valid lives could not be obtained due to the extremely long lives and insufficient failures during the test program. It appeared that a vital element in this improved life was a reduced infeed during the final diamond finish grinding. More work would be necessary to confirm this however. Acceptably smooth finishes with equivalently excellent fatigue life were obtained with light grinding with silicon carbide wheels. This is an important development as it allows more economical production of crowned geometries on silicon nitride bearing rollers by the use of formed silicon carbide wheels. The exceptionally long rolling contact fatigue life of these specimens demonstrates the need for the development of an accelerated ceramic bearing material testing procedure and its correlation with actual bearing performance as well as material properties, surface characterization, and defect morphologies.

ABSTRACT

Strength, surface finish and rolling contact fatigue life were determined on two grades of hot pressed silicon nitride after a total of twenty-seven different surface finishing procedures. Rolling contact fatigue lives of silicon nitride with selected smoother finishes tested at 800 ksi Hertz stress were an order of magnitude longer than those obtained on the M50 bearing steel controls and more than twice as long as the best results previously obtained on silicon nitride.

FOREWORD

This report was prepared by Industrial Ceramics Division, Norton Company under Army Materials and Mechanics Research Center contract DAAG46-74-C-0055 and covers the work performed during the period January 1974 through July 1975. This report is the final report and summarizes all activities under the contract. This project was funded by the U. S. Army Troop Support Command under Project No. 7745506. The AMMRC Technical Monitor for this contract was G. M. Harris. The TROSCOM Monitor was E. York.

CONTENTS

LIST OF FIGURES

LIST OF FIGURES
CONTINUED

LIST OF TABLES

I INTRODUCTION

Previous studies[1,3,4] have shown that hot pressed silicon nitride has rolling contact fatigue lives several times those of the high performance bearing steel CVM M50 and these results have been largely confirmed by the actual bearing tests run to date on bearings of both all silicon nitride and silicon nitride rollers in M50 races.[3,4] As noted below, early results have shown the importance of finishing procedures upon rolling contact fatigue (RCF) test lives. However, no study had been carried out to optimize these finishing techniques. Accordingly this program was begun to optimize this vital element of finishing procedures for production of the longest possible fatigue lives for silicon nitride roller bearing elements.

Previous rolling contact fatigue (RCF) studies on silicon nitride have shown that the finishing methods used to prepare the bearing surface have a significant effect on the ceramic fatigue life.[1,2] For example, specimens ground with a 320 grit diamond wheel to an eight microinch surface roughness had a median fatigue life approximately 500 times longer than specimens that were initially ground with a 100 grit diamond wheel and subsequently diamond lapped to a three microinch finish. The predominant failure mode in RCF studies[3,4] of dense, low inclusion content silicon nitride is spalling induced by Hertzian crack formation. The Hertzian cracks are presumed to initiate from pre-existing surface flaws on the material. Therefore, the degree of perfection, i.e. the presence or severity of surface flaws, is expected to influence strongly the performance life of ceramic materials. Since the strength of brittle materials is frequently controlled by surface flaws, a measure of material strength indicates the severity of the surface flaws.

The surface roughness of a bearing component influences the type of lubrication possible at the contact. For rough bearing surfaces, the bearing load is carried by surface asperities and boundary lubrication prevails. Lower wear, friction and heat generation result if elastohydrodynamic (EHD) lubrication exists at the contact. Full EHD lubrication is characterized by a continuous oil film between the mating surfaces. It is possible to estimate the degree of asperity interaction by considering the ratio of the lubrication film thickness, h, to the composite roughness, r, of the contacting surfaces.[5] The composite roughness is defined as the square root of the sum of the squared root mean square (rms) roughness of the two contacting surfaces. For values of $h/r \geq 3.5$, a fully continuous EHD film exists. As the ratio decreases, film effectiveness decreases until at $h/r \leq 1$, the load is mainly carried by touching asperities. Well lubricated steel/silicon nitride contacts are especially important. Because of the high hardness of silicon nitride, inadequate lubrication of these contacts can cause premature fatigue of the steel contact component.[6]

The current program was undertaken to develop the manufacturing technology for optimization of silicon nitride finishing techniques to maximize ceramic bearing performance. Twenty-seven finishing procedures were used to generate surfaces on hot pressed silicon nitride. These surfaces were screened for bearing suitability by means of strength and surface roughness characterization. A smaller number of selected finishes were then evaluated in rolling contact fatigue studies to further define the optimum finishing procedures.

II MATERIAL DESCRIPTION AND CHARACTERIZATION

Two types of hot-pressed silicon nitride, Norton Company HS-110 and NC-132, were evaluated in the program. The NC-132 silicon nitride is of higher chemical purity which results in a smaller amount of the intergranular bonding phase and improved mechanical properties, especially at temperatures in excess of 1100°C. Since it is known that the relatively higher inclusion content of normal HS-110 silicon nitride material promotes inclusion initiated bearing failures[1] and since the current program is intended to investigate the effect of finishing on ceramic life, the starting powder of the HS-110 billet was additionally processed to reduce the inclusion level to approximately that of the NC-132 material. One HS-110 and two NC-132 silicon nitride billets, of dimensions 15 cm X 15 cm X 2.5 cm (6 inch X 6 inch X 1 inch) were hot pressed, characterized and subsequently used in the program.

The major metallic impurities in the billets, as determined by emission spectrography, are presented in Table I, along with billet densities. It is seen that the HS-110 billet is significantly higher in Al, Fe and Ca. The billets were x-rayed and the negatives examined to ensure the absence of large inclusions and density variations.

TABLE I

Billet Analyses and Densities

Billet	Element (weight percent) Al	Ca	Fe	Mg	W	Density (g/cc)
HS-110	0.40	0.22	1.14	0.72	3.9	3.23
NC-132 (A)	0.20	0.05	0.40	0.70	2.7	3.23
NC-132 (B)	0.20	0.05	0.64	0.74	2.6	3.24

Billet strengths were evaluated by bend testing to provide an additional quality control check and reference strength levels.

Rectangular bar specimens were sliced and diamond ground from the billet stock. The specimen size for the NC-132 bend bars was 0.318 cm X 0.635 cm X 5.08 cm (1/8 inch X 1/4 inch X 2 inch), while that for the HS-110 bars was 0.318 cm X 0.318 cm X 5.08 cm (1/8 inch X 1/8 inch X 3 inch). The bars were wet finish ground with a 320 diamond grit wheel such that the grinding scratches were parallel to the long axis of the bar. The specimen edges were ground with a 45°, 0.013 cm (0.005 inch) bevel to suppress edgeflaw breaks during strength testing.

The bars were broken in four-point bending with an Instron mechanical test machine at a crosshead speed of 0.051 cm/min (0.020 inch/min). The upper and lower spans of the bend test fixture were 1.91 cm (0.75 inch) and 3.81 cm (1.50 inch), respectively. All bars were broken in the "strong" orientation (the hot pressing direction in the material was parallel to the applied force direction in the bend test) and the NC-132 specimens were broken in the plate configuration. Material bend strengths were computed from the four-point formula:

$$\sigma_f = \frac{3Pa}{bd^2} \qquad \text{Eqn 1}$$

where, σ_f = fracture stress

P = fracture load

a = moment arm

b = sample width

d = sample thickness

The bend test data are presented in Table II and are within the normal strength variations for these materials.

III PREPARATION AND INITIAL EVALUATION OF MATERIAL FINISHES

A. Sample Preparation

A total of twenty-five finishes were applied to bend rods cut from the NC-132(B) silicon nitride billet. Bars, 15 cm long, were sliced from the billet and surface ground into hexagonal prisms. The bars were wet ground to oversized rounds using a 150 grit diamond wheel (specification SD150-R75B69) on a cylindrical grinder with a steady rest. The rods were then cut to 5.1 cm lengths and randomly divided in 25 groups of 8 rods each. The details of the subsequent finishing steps that were used to prepare the different finishes are listed in Table III, where they are grouped according to the nature of the last finishing operation. All of the grinding and finishing steps described were carried out at the Norton Company with the exception of the

TABLE II

Billet 4-point Bend Strengths

Break #	Billet Strength MN/m^2, (ksi) HS-110	NC-132(A)	NC-132(B)
1	807,(117)	750,(109)	931,(135)
2	889,(129)	765,(111)	917,(133)
3	910,(132)	807,(117)	965,(140)
4	889,(129)	827,(120)	869,(126)
5	952,(138)	834,(121)	938,(136)
6	938,(136)	703,(102)	841,(122)
7	669,(97)	952,(138)	1000,(145)
8	883,(128)	972,(141)	1007,(146)
9	958,(139)	1020,(148)	931,(135)
10	1007,(146)	758,(110)	917,(133)
11	869 (126)	--	--
12	476 (69)	--	--
Mean Strength	855 (124)	841 (122)	931 (135)
Standard Deviation	145 (21)	103 (15)	52 (7.6)

TABLE III

NC-132 Strength Rod Finishing Procedures

	Finish Variation	Finish Step #	Wheel (or abrasive) Specification	Total Diametral Stock Removal of Step (0.001 cm)	Work Traverse Rate (cm/min)	Diametral Stock Removal Per Pass (0.001 cm)
I.	DIAMOND GRINDING WHEEL FINAL FINISHES					
	1	1	SD150-R75B69	25.4	64	2.54
	2	1	SD150-R75B69	25.4	64	2.54
		2	SD220-N75B69	20.3	32	2.54
	3	1	SD150-R75B69	25.4	64	2.54
		2	SD320-R75B69	5.08	32	2.54
	4	1	SD150-R75B69	25.4	64	2.54
		2	SD320-R75B69	15.24	32	2.54
	5	1	SD150-R75B69	25.4	64	2.54
		2	SD320-R75B69	25.4	32	2.54
	6	1	SD150-R75B69	25.4	64	2.54
		2	SD220-N75B69	15.24	32	2.54
		3	SD320-R75B69	5.08	32	2.54
	7	1	SD150-R75B69	25.4	64	2.54
		2	SD220-N75B69	15.24	32	2.54
		3	SD320-R75B69	15.24	32	2.54
	8	1	SD150-R75B69	25.4	64	2.54
		2*	SD320-R75B69	25.4	32	2.54
	9	1	SD150-R75B69	25.4	64	2.54
		2	SD320-R75B69	25.4	32	3.81
	10	1	SD150-R75B69	25.4	64	2.54
		2	SD320-R75B69	15.24	32	1.27

continued

TABLE III (continued)

Finish Variation	Finish Step #	Wheel (or abrasive) Specification	Total Diametral Stock Removal of Step (0.001 cm)	Work Traverse Rate (cm/min)	Diametral Stock Removal Per Pass (0.001 cm)
II. SILICON CARBIDE GRINDING WHEEL FINAL FINISHES					
11	1	SD150-R75B69	25.4	64	2.54
	2	SD320-R75B69	20.32	32	2.54
	3	37C150-M7VK	2.54	32	1.27
12	1	SD150-R75B69	25.4	64	2.54
	2	SD320-R75B69	20.32	32	2.54
	3*	37C150-R8BH	$\sim$0.51	32	$\ll$1
13	1	SD150-R75B69	25.4	64	2.54
	2	SD320-R75B69	20.32	32	2.54
	3	37C150-R8BH	2.54	32	1.27
14	1	SD150-R75B69	25.4	64	2.54
	2	SD320-R75B69	20.32	32	2.54
	3	37C150-R8BH	7.62	32	1.27
III. DIAMOND HONE FINAL FINISHES					
15	1	SD150-R75B69	25.4	64	2.54
	2	SD320-R75B69	20.32	32	2.54
	3	400 grit hone	1.02	-	-
16	1	SD150-R75B69	25.4	64	2.54
	2	SD320-R75B69	20.32	32	2.54
	3	400 grit hone	2.03	-	-
17	1	SD150-R75B69	25.4	64	2.54
	2	SD320-R75B69	20.32	32	2.54
	3	600 grit hone	1.02	-	-
18	1	SD150-R75B69	25.4	64	2.54
	2	SD320-R75B69	20.32	32	2.54
	3	400 grit hone	1.02	-	-
	4	600 grit hone	1.02	-	-

continued

TABLE III (continued)

Finish Variation	Finish Step #	Wheel (or abrasive) Specification	Total Diametral Stock Removal of Step (0.001 cm)	Work Traverse Rate (cm/min)	Diametral Stock Removal Per Pass (0.001 cm)
IV. LAPPING FINAL FINISHES					
19	1	SD150-R75B69	25.4	64	2.54
	2	SD320-R75B69	20.32	32	2.54
	3	Lapped with 6 micron diamond paste**	1.52	-	-
20	1	SD150-R75B69	25.4	64	2.54
	2	SD320-R75B69	20.32	32	2.54
	3	Lapped with 600 grit B_4C water slurry***	1.78	-	-
21	1	SD150-R75B69	25.4	64	2.54
	2	SD320-R75B69	20.32	32	2.54
	3	Lapped with 1000 grit SiC water slurry***	1.27	-	-
22	1	SD150-R75B69	25.4	64	2.54
	2	SD320-R75B69	20.32	32	2.54
	3	Lapped with 6 micron diamond paste**	1.52	-	-
	4	Lapped with SnO_2 water slurry**	nil	-	-
23	1	SD150-R75B69	25.4	64	2.54
	2	SD320-R75B69	20.32	32	2.54
	3	Lapped with 6 micron diamond paste**	1.52	-	-
	4	Lapped with CeO water slurry**	nil	-	-

continued

TABLE III (continued)

Finish Variation	Finish Step #	Wheel (or abrasive) Specification	Total Diametral Stock Removal of Step (0.001 cm)	Work Traverse Rate (cm/min)	Diametral Stock Removal Per Pass (0.001 cm)
V. OTHER FINAL FINISHES					
24	1	SD150-R75B69	25.4	64	2.54
	2	SD320-R75B69	15.24	32	2.54
	3	Tumbled 24 hours in 100 grit B_4C***	nil	-	-
25	1	SD150-R75B69	25.4	64	2.54
	2	SD320-R75B69	20.32	32	2.54
	3	Hot fluorine gas etch****	variable	-	-

NOTES: Metric dimensions converted from English units; 1 cm = 2.54 inch

* Wheel speed = 2895 surface meters per minute (SMPM)

** Abrasive from Buehler Ltd, Evanston, Ill.

*** Abrasive from Norton Company, Worcester, MA.

**** Gas polishing performed at Naval Research Laboratory. See references 7 and 8 for details of technique.

lapping operations which were carried out by Westfield Gage Company, Westfield, MA, and the gas polishing finishing carried out by the Naval Research Laboratory. Final specimen size was 0.476 cm diameter X 5.1 cm long (3/16 inch diameter X 2 inch).

Variables in the finishing procedures include 1) method of imparting final finish (grinding, honing, lapping, tumbling, gas polishing), 2) abrasive type (diamond and silicon carbide wheels and various lapping compounds), 3) depth of material removed per finishing step, 4) abrasive grit size, 5) abrasive bond type and grade hardness, and 6) grinding wheel speed. All specimen grinding reported in Table III was performed on a Ded-Tru* centerless cylindrical grinding attachment mounted on the bed of a surface grinder. All grinding was done wet with a 2 percent water solution of Norton Wheelmate 203 coolant, and, with the two noted exceptions, at a peripheral wheel speed of 1675 surface meters per minute (SMPM).

All of the diamond grit abrasive wheels (specifications beginning with the letters SD followed by the grit size) were phenolic bonded as previous experience has shown that grinding silicon nitride with metal bonded diamond wheels frequently results in surface damage from thermal shocking. Both the glass bonded (37C150-M7VK) and the phenolic bonded (37150-R8BH) 150 grit silicon carbide wheels wore rapidly during grinding and had to be dressed frequently to maintain stock removal rates and wheel face condition. During grinding with the glass bonded silicon carbide wheel, small clumps of bond and abrasive broke from the wheel and tended to lodge between the work and the work blade rest producing an undesireable chatter effect. At the higher wheel speed of 2895 SMPM, extremely rapid wear of the silicon carbide grits glazed the wheel and resulted in minimal stock removal. The rapid formation of flat areas on the silicon carbide grits results from the roughly equivalent hardnesses ($\sim 2500/mm^2$) of silicon carbide and silicon nitride. Abrasive flat formation greatly increases the frictional heat generated in grinding and can produce thermal shock damage in silicon nitride workpieces. Although silicon carbide grinding has been found useful in producing crowned contours on silicon nitride bearing rollers, the use of silicon carbide wheels to grind silicon nitride is recommended for stock removals less than approximately 0.003 cm and then only with frequent wheel dressings.

The hone finishes were performed manually on an external Sunnen† hone using diamond hones with oil lubricant. The lapped finishes were done with hand held, cast iron ring laps and the appropriate abrasive. The boron carbide abrasive removed material faster than the other lapping compounds, while the relatively soft tin oxide and cerium oxide abrasives removed negligible material and were useful for polishing purposes only.

---

* Unison Corp, Madison Heights, MI
† Sunnen Company, St. Louis, MO

A micrometer was used to measure stock removals greater than 0.00254 cm. To measure stock removals less than this, an electronic indicating gage and a mechanical dial indicator gage with marble table were used for the lapping and honing removals, respectively.

B. Surface Roughness Measurements

The Arithmetic Average (AA) surface roughness values for the finishing variations were measured parallel to the specimen axis on a Bendix Profilometer* with a 0.076 cm (0.030 inch) cut-off and are recorded in Table IV. The average roughness for a given finish is the average of eight measurements, one from each member of the finish group.

C. Strength Testing of Finishes

The specimen rods were broken in three-point bending over a span of 4.45 cm (1.75 inch) and at an Instron crosshead rate of 0.051 cm/min (0.020 inch/min). Modulus of rupture values were calculated from the circular beam formula:

Eqn 2

$$\sigma_f = PL/\pi R^3$$

where, σ_f = fracture stress

P = fracture load

R = beam radius

The average strength and its standard deviation for the finishes are listed in Table V. Eight specimens per finish were broken, with the exception of Variation 25 for which only two rods were suitable. The other five rods were etched under modified conditions which produced a non-uniform rod cross-section.

An examination of the fracture surfaces by low-power optical microscopy showed, as well as could be determined at the low magnification, that the fractures originated exclusively at the rods' circumferences. If internal fracture origins were existent, it is believed that some internal origins would have been observed at these modulus of rupture values. The absence of internal fracture origins indicates that the fractures were exclusively initiated by surface flaws.

D. Discussion of Strength Rod Finishes

The correlation between bend strength and surface roughness for the specimens is shown in Figure 1. As anticipated[9], the bend strength increases with greater surface smoothness implying a reduction in the severity of surface flaws. Certain details of the correlation were, however, unexpected.

* Bendix Corp., Dayton, OH

TABLE IV

Finish Roughness Values, meters x 10^{-8}, AA (microinches, AA)

Finish Variation	Average Roughness	Roughness Range
1	91.4, (36.0)	81-102, (32-40)
2	63.5, (25.0)	56-74, (22-29)
3	36.8, (14.5)	36-38, (14-15)
4	38.9, (15.3)	38-41, (15-16)
5	38.9, (15.3)	38-41, (15-16)
6	43.2, (17.0)	41-46, (16-18)
7	41.9, (16.5)	41-43, (16-17)
8	36.6, (14.4)	33-41, (13-16)
9	39.6, (15.6)	38-43, (15-17)
10	35.0, (13.8)	33-41, (13-15)
11	15.7, (6.2)	13-18, (5-7)
12	26.6, (9.3)	18-30, (7-12)
13	12.9, (5.1)	8-20, (3-8)
14	17.5, (6.9)	13-25, (5-10)
15	19.6, (7.7)	8-27, (3-10.5)
16	9.9, (3.9)	8-15, (3-6)
17	7.1, (2.8)	6.4-8.1, (2.5-3.2)
18	7.1, (2.8)	5.6-11.4, (2.2-4.5)
19	2.8, (1.1)	2.5-3.3, (1.0-1.3)
20	5.8, (2.3)	3.0-7.9, (1.2-3.1)
21	4.1, (1.6)	3.0-6.1, (1.2-2.4)
22	1.2, (0.49)	1.0-2.0, (0.40-0.80)
23	1.4, (0.55)	1.3-1.5, (0.50-0.60)
24	49.8, (19.6)	40-61, (16-24)
25*	73.7, (29.0)	- - - - -

*Two specimens only

TABLE V

Surface Bend Strengths

Finish Variation	Average Strength MN/m^2 , (ksi)	Standard Deviation MN/m^2 , (ksi)
1	391 , (56.7)	15.7 , (2.28)
2	432 , (62.6)	24.1 , (3.50)
3	527 , (76.5)	31.4 , (4.56)
4	565 , (81.9)	41.1 , (5.96)
5	525 , (76.2)	23.0 , (3.34)
6	566 , (82.1)	32.1 , (4.65)
7	562 , (81.5)	23.0 , (3.34)
8	622 , (90.2)	30.4 , (4.41)
9	542 , (78.6)	30.2 , (4.38)
10	565 , (81.9)	41.1 , (5.96)
11	565 , (82.0)	66.4 , (9.63)
12	608 , (88.2)	74.5 , (10.8)
13	618 , (89.6)	55.2 , (8.01)
14	654 , (94.8)	103. , (14.9)
15	540 , (78.3)	47.1 , (6.83)
16	675 , (98.0)	67.4 , (9.78)
17	662 , (96.0)	59.2 , (8.58)
18	698 , (101.2)	126. , (18.3)
19	798 , (115.8)	87.6 , (12.7)
20	705 , (102.2)	86.2 , (12.5)
21	714 , (103.6)	96.5 , (14.0)
22	672 , (97.4)	65.2 , (9.45)
23	665 , (96.5)	65.8 , (9.54)
24	507 , (73.5)	32.9 , (4.77)
25*	728 , (105.6)	- - - -

*Two breaks only : 678 and 778 MN/m^2

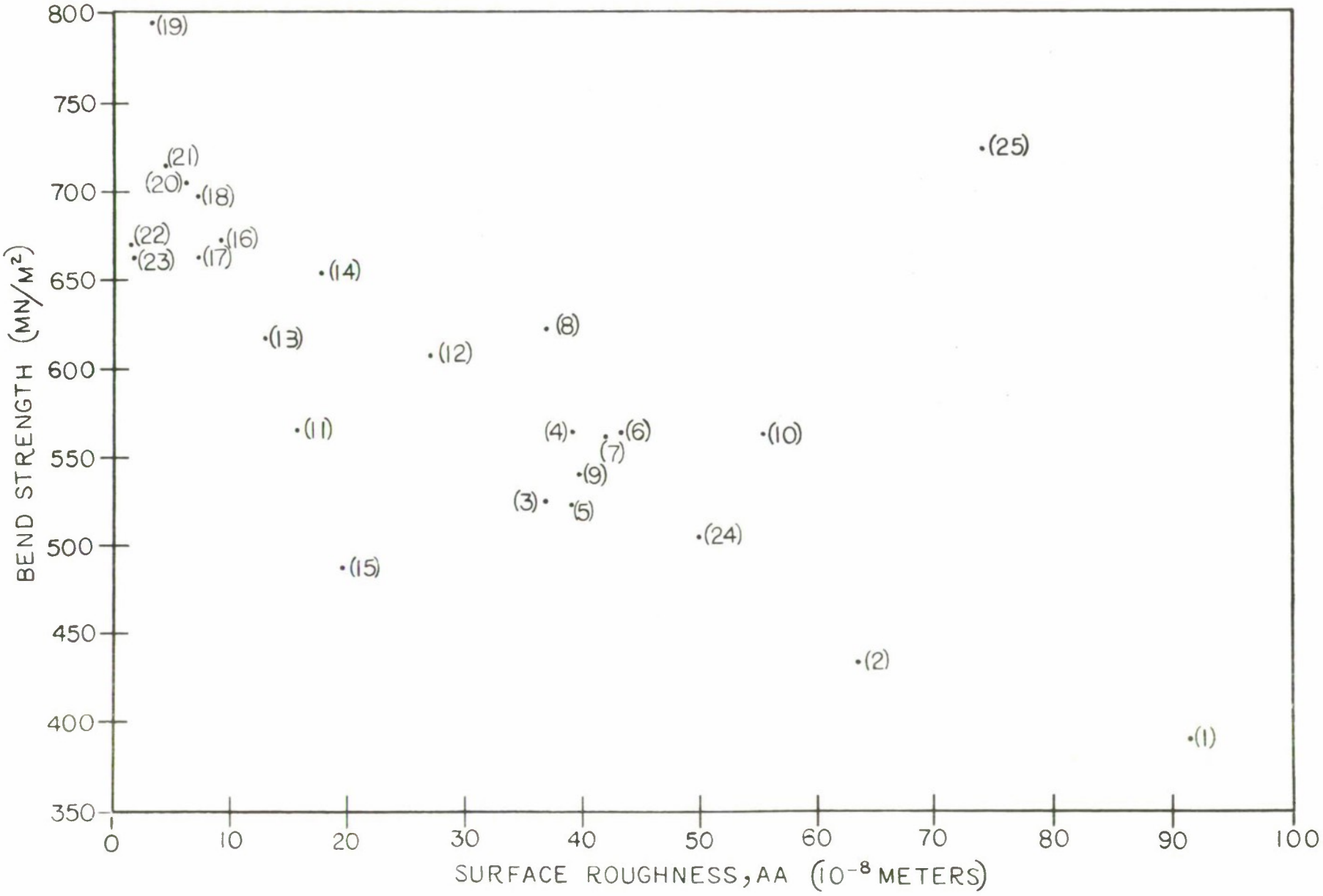

FIGURE 1 - Strength vs. Roughness for finishing variations

It had been anticipated that the stress intensity factor for the surface flaws associated with the smoother surfaces would eventually fall below that for inherent internal flaws, at which point the strength would plateau at a constant value. Furthermore, because of the smoother finishes and the smaller stressed volume of the three-point versus the four-point bend test, it was expected that the highest strengths of the round rods would be in excess of the 931 MN/m^2 (135 ksi) strength obtained for billet qualification. Neither expectation was realized.

The absence of the expected behavior can be explained on the basis of retained grinding damage from previous finishing steps. Repeated diameter measurements on ground specimens revealed that the rods were frequently out of round by about 1-2 x 10^{-3} cm (0.0005 inch), a significant amount because stock removal steps subsequent to grinding were of this magnitude and the lapping and honing operations could not be expected to remove a uniform layer of material from a non-uniform cross section. Microscopic examination of lapped or honed specimens revealed traces of grinding scratches. Retained grinding damage is also reflected in the relatively higher coefficients of variation for the strengths and range of roughnesses for the smoother finishes. It is concluded that the strengths of all of the honed and lapped finishes are below their potential strengths.

The orientation of the flaws associated with the grinding scratches with respect to the applied tensile bending stresses further helps to explain the lower strengths of the three-point results. In the four-point test, the scratches were parallel to the stress vector, while in the three-point test the scratches are circumferential and, therefore, perpendicular to the stress. An indication of the effect of flaw orientation on strength may be obtained by comparing the respective 320 grit diamond wheel finish strengths; the three-point bend specimens had a 550 MN/m^2 (80 ksi) strength as compared to the 930 MN/m^2 (135 ksi) four-point values.

Similar conclusions pertaining to residual damage in the smoother finished are reached when one considers a fracture mechanics approach to the depth of damage. The depth of surface damage may be estimated from the strength by means of the relation:

$$K_{I_c} = 1.12\,\sigma_f\,(\pi a)^{1/2} \qquad \text{Eqn 3}$$

where, K_{I_c} = critical stress intensity factor for silicon nitride

$= 4.7\ MN/m^{3/2}$ (Reference 10)

σ_f = fracture strength

and a = flaw depth,

if the surface flaws can be treated as microcracks, as has been shown to be the case for ground surfaces.[9] Table VI presents the calculated effective flaw depths for a series of finishes of different strengths. Also tabulated is the ratio of flaw size to the corresponding roughness value.

TABLE VI

Strength vs Calculated Flaw Size for Bend Specimens

Finish Variation	Strength MN/m^2	Flaw Size 10^{-6} m	Flaw Size/ AA value
1	391	36.6	40
2	432	30.0	47
7	562	17.7	42
12	608	15.2	57
17	662	12.8	180
21	714	11.0	268

The calculated flaw sizes are much greater than the surface roughness, indicating that the surface damage includes true microcracks which extend far below the external surface. The flaw-to-roughness ratio is relatively constant for the diamond ground finishes and increases for the smoother, non-ground final finishes. At least part of this increase is attributable to retained grinding damage. Taking 550 MN/m^2 (80 ksi) as a representative strength for the specimens finished with a 320 diamond grit grinding wheel, the corresponding flaw depth is 18 micrometers. This depth is greater than the typical surface layer (5-10 micrometers) removed by the lapped and honed finishes.

Turning to a discussion of specific finishing procedures, the benefits of using a relatively fine diamond grit wheel to finish grind silicon nitride, such as a 320 grit wheel, as opposed to using a roughing wheel, such as a 220 or 150 grit wheel, is readily seen in the strength and surface finish improvements. The removal of as little as 0.0025 cm (0.001 inch) from a surface with a 320 grit wheel is sufficient to remove the damage of a 150 or 220 grit wheel to a level no greater than that of the 320 wheel itself. All of the 320 grit diamond final grind finishes (Variations 3, 4, 5, 6, 7, 9 and 10) are basically similar with respect to strength and roughness and small changes in the feeds and traverse rates did not make large differences. An exception to

this uniformity is Variation 8, wherein the wheel speed was increased from the standard 1675 SMPM to 2895 SMPM, which resulted in a strength increase.

The 150 grit silicon carbide wheels (Variations 11 - 14) produced smoother and generally stronger finishes than the 320 grit diamond wheel. Despite the larger grit size of the silicon carbide, these results are believed traceable to the smaller grit penetration of the rapidly wearing silicon carbide grits. As has been shown,[2] the silicon carbide abrasives produce a distinctly different surface appearance than diamond grinding. (Representative micrographs of the various finishes are presented in Section V.) The rapid wear of the silicon carbide grits rules out the practical use of silicon carbide wheels for major stock removal and can produce thermal shock damage, even for minor stock removals, if the wheel is not frequently dressed. The relatively lower strength of the glass bonded silicon carbide wheel (specification 37C150-M7VK, Variation 11) is believed to be associated with additional damage caused by the wheel wear in the form of clumps of bond and abrasive which produced an uneven grinding action. This type of wheel wear could be theoretically suppressed by using a vitrified wheel with a higher glass bond content. The phenolic resin bonded silicon carbide wheel (specification 37C150-R8BH, Variations 12-14) produced higher strengths than the glass bonded silicon carbide wheel. When the phenolic wheel (Variation 12) was run at the higher wheel speed, grit penetration and stock removal essentially stopped as the wheel glazed rapidly.

The retention of residual grinding damage in the honed and lapped finishes are especially evident in Variation 15, whose strength remained at the 320 grit diamond grinding level. Both diamond honing and abrasive lapping are capable of producing very smooth surfaces on silicon nitride, with the smoothest surfaces produced by the tin and cerium oxide polishing compounds (Variations 22 and 23). Since these soft materials could not abrade the silicon nitride, diamond paste lapping was used to remove the majority of the 320 grit diamond wheel damage prior to their use. The oxide polished specimens had lower strengths than that of the straight diamond paste lapped samples (Variation 19), but this discrepancy is most probably due to uncertanties in small levels of stock removal. The already noted relatively fast lapping stock removal by the boron carbide abrasive is related to its low strength and high friability which ensures a fresh supply of sharp cutting points. However, this attribute was not effective in Variation 24, which demonstrated the inappliability of tumbling as a finishing procedure for silicon nitride.

The strength of the gas etched rods was considerably higher than for a ground surface of equivalent roughness. The etch pitted the silicon nitride and increased the roughness, but, because of the nature of the etch, sharp flaws were not introduced.

IV ROLLING CONTACT FATIGUE TESTING

A. Introduction

Based upon the strengths and surface finishes produced on the strength rods, a reduced number of finishes were selected for application to rolling contact fatigue (RCF) specimens of two grades of silicon nitride. In general, the selected finishes, Table VIII, represent a variety of machining methods but possess above average strength and smoothness. The specimens were characterized with respect to geometrical perfection, surface roughness and microscopic appearance. After RCF testing, the specimens were again examined by microscopy.

B. Specimen Preparation

Two grades of hot pressed silicon nitride, HS-110 and NC-132, were used for the preparation of the RCF specimens. The billet materials have been characterized in Section II. The RCF specimen geometry is a straight cylindrical rod of 0.9520 ±0.0005 cm (0.3748 ±0.0002 inch) diameter, nominal length 7.6 cm (3 inch) and a maximum out of roundness specification of 1.27×10^{-4} cm (50×10^{-6} in). The latter criterion is intended to ensure a minimal vibration and constant maximum contact stress during fatigue testing.

Grinding was initially attempted on the grinding attachment used to prepare the strength test rods. However, because of the limited number of samples for a given surface preparation (which requires machine adjustments), it was not possible to set up the machine correctly for a given finish. As a result, it was not possible to meet the out of roundness specification for the specimens by this method. An example of a rejected out of round geometry is shown in the polar chart, Figure 2.

To overcome the out-of-roundness problem, the method of specimen fabrication was altered. Specimen rod blanks were prepared by rough grinding to a 0.025 cm oversized diameter. Steel dead centers were epoxied to ends of the 7.6 cm blanks for subsequent grinding on a standard cylindrical grinder. The preparation of all finishes required additional grinding, the conditions of which are listed in Table VII. The switch in the grinding machine type (from centerless to cylindrical) necessitated some changes in machining parameters of the RCF specimens, as compared to those of the strength rod specimens. The most notable example of this was the change in infeeds during final diamond grinding to ensure specimen roundness.

A total of thirty RCF specimens were prepared; ten of HS-110 material and twenty of NC-132 material. Counting material type as a variable, fifteen distinct finishes were employed, with a

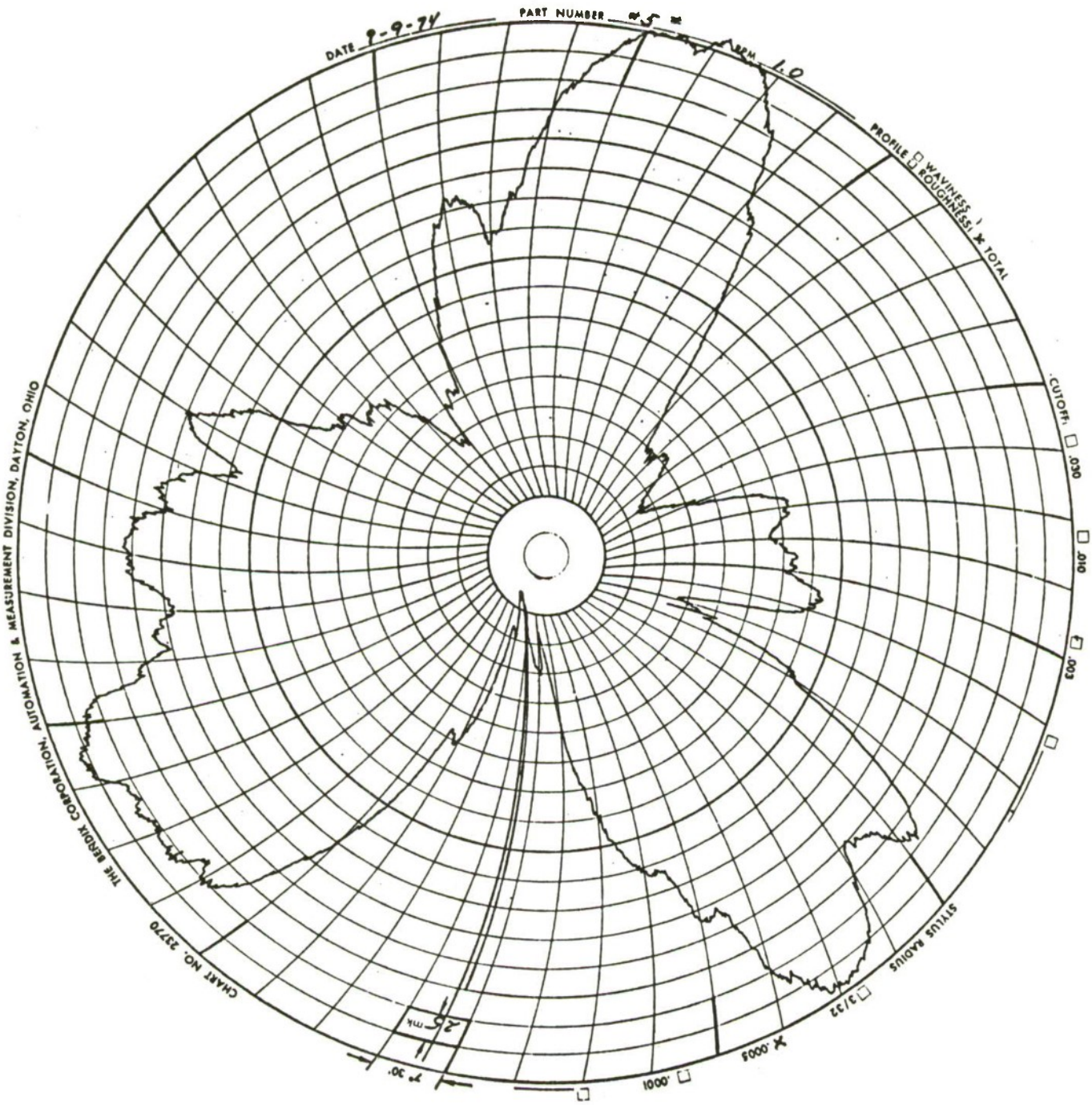

FIGURE 2 - Polar chart of reject RCF rod

TABLE VII

Grinding Conditions for RCF Rod Specimens
After Initial Roughing of Blanks

Machine	Brown and Sharpe #5 Cylindrical
Coolant	1 part Houghton Hicut #3210 to 50 parts water
Wheel Speed	1675 SMPM
Traverse Rate	Manual
Work Speed	Diamond wheels - 319 RPM Silicon carbide wheels - 202 RPM
Stock Removal	Diamond wheels - Radial infeed was 0.0013 cm (0.0005 inch) per pass during grinding to within 0.0038 cm (0.0015 inch) oversize and 0.00025 cm (0.0001 inch) per pass during final grinding. Silicon carbide - Wheel breakdown caused uncertainty in true infeed rate.

duplicate specimen for each finish. Table VIII describes the finishing variations applied to the RCF specimens after blank fabrication. All finish grinding and the lapping operations were performed at Westfield Gage, Inc., Westfield, MA, according to Norton Company specifications. The honing operations were performed at Norton Company. Four of the five HS-110 material finishes were also applied on the NC-132 material in order to evaluate the effect of material type. The number system used for the related strength rod finishes has been retained and two new finishes (#26 and #27) have been incorporated to study further the effects of honing.

C. Metrology of RCF Specimens

The fabricated RCF specimens were measured for axial surface and, at each end, for circumferential surface finish and roundness. These values are presented in Table IX. The specimens exhibited some of the most perfect geometries for a bearing component ever evaluated at the Federal Mogul Research Laboratory, with the possible exception of Grade 10, or better, steel balls. Some rods were round to within 0.25 microns (10^{-5} inch) and with surface roughnesses as low as 0.0025 microns, AA (10^{-7} inch, AA), which exceeded the ability of the instrument to be measured accurately. Figure 3 is a polar chart of one of the more round rods of the program. In previous RCF testing of silicon nitride,

TABLE VIII

Finishing procedures for RCF rod specimens

Finish Variation	Finish Step #	Wheel (or abrasive) Specification	Rod Code #	Rod Diameter After Step cm, (inch)
I. HS-110 Si_3N_4 Finishes				
5	1	SD320-R100B69	8	0.9523, (0.3749)
			8A	0.9523, (0.3749)
14	1	SD320-R100B69	9	0.9548, (0.3759)
			9A	0.9548, (0.3759)
	2	37C150MVK	9	0.9520, (0.3748)
			9A	0.0523, (0.3749)
17	1	SD320-R100B69	18	0.9533, (0.3753)
			18A	0.9533, (0.3753)
	2	600 grit hone	18	0.9522, (0.3749)
			18A	0.9520, (0.3748)
19	1	SD320-R100B69	12	0.9533, (0.3753)
			12A	0.9533, (0.3753)
	2	Lapped with 6 micron diamond paste	12	0.9523, (0.3749)
			12A	0.9520, (0.3748)
23	1	SD320-R100B69	13	0.9530, (0.3752)
			13A	0.9533, (0.3753)
	2	Lapped with 6 micron diamond past	13	0.9522, (0.37488)
			13A	0.9521, (0.37486)
	3	Lapped with CeO water slurry	13	0.9521, (0.37486)
			13A	0.9521, (0.37484)

Continued

TABLE VIII (continued)

Finishing procedures for RCF rod specimens

Finish Variation	Finish Step #	Wheel (or abrasive) Specification	Rod Code #	Rod Diameter After Step cm, (inch)
II. NC-132 Si_3N_4 Finishes				
5	1	SD320-R100B69	10	0.9520, (0.3748)
			10A	0.9520, (0.3748)
14	1	SD320-R100B69	11	0.9550, (0.3760)
			11A	0.9550, (0.3760)
	2	37C150MVK	11	0.9520, (0.3748)
			11A	0.9523, (0.3749)
15	1	SD320-R100B59	19	0.9533, (0.3753)
			19A	0.9533, (0.3753)
	2	400 grit hone	19	0.9520, (0.3748)
			19A	0.9520, (0.3748)
17	1	SD320-R100B69	20	0.9533, (0.3753)
			20A	0.9533, (0.3753)
	2	600 grit hone	20	0.9520, (0.3748)
			20A	0.9520, (0.3748)
19	1	SD320-R100B69	14	0.9533, (013753)
			14A	0.9533, (0.3753)
	2	Lapped with 6 micron diamond paste	14	0.9517, (0.3747)
			14A	0.9523, (0.3749)
20	1	SD320-R100B69	15	0.9530, (0.3752)
			15A	0.9530, (0.3752)
	2	Lapped with 600 grit B_4C	15	0.9520, (0.3748)
			15A	0.9520, (0.3748)
21	1	SD320-R100B69	16	0.9533, (0.3753)
			16A	0.9533, (0.3753)
	2	Lapped with 1000 grit SiC	16	0.9523, (0.3749)
			16A	0.9523, (0.3749)

Continued

TABLE VIII (continued)

Finishing procedures for RCF rod specimens

Finish Variation	Finish Step #	Wheel (or abrasive) Specification	Rod Code #	Rod Diameter After Step cm, (inch)
22	1	SD320-R100B69	17	0.9533, (0.3753)
			17A	0.9533, (0.3753)
	2	Lapped with 6 micron diamond paste	17	0.9521, (0.37484)
			17A	0.9521, (0.37483)
	3	Lapped with SnO_2 water slurry	17	0.9521, (0.37483)
			17A	0.9520, (0.37482)
26	1	SD150-R75B69	21	0.9533, (0.3753)
			21A	0.9535, (0.3754)
	2	600 grit hone	21	0.9522, (0.3749)
			21A	0.9520, (0.3748)
27	1	SD220-R75B69	22	0.9530, (0.3752)
			22A	0.9528, (0.3751)
	2	600 grit hone	22	0.9530, (0.3746)
			22A	0.9517, (0.3747)

TABLE IX

RCF Specimen Geometry

Rod Code	Axial Surface Finish (micro in. AA)	Coded End		Plain End	
		Circumferential Surface Finish (micro in. AA)	Roundness (in. x 10^{-6})	Circumferential Surface Finish (micro in. AA)	Roundness (in. x 10^{-6})
8	10 - 12	8 - 9.5	< 50	7.5 - 8.5	< 50
8A	11 - 13	8 - 9.5	< 50	7 - 8.5	< 50
9	1 - 2	1 - 2	< 50	1 - 2	< 50
9A	1 - 1.5	1.5 - 2	< 50	1.5 - 2	< 50
10	12 - 13	8 - 9	< 50	8 - 10	< 50
10A	12 - 13	9 - 10.5	< 50	9 - 10	< 50
11	0.5 - 1.5	1 - 2	< 50	1 - 2	< 50
11A	1 - 1.5	1 - 2	< 50	1 - 2	< 50
12	0.6 - 1.2	2 max.	< 10	2 max.	< 10
12A	0.6 - 1.2	2 max.	< 10	2 max.	< 10
13	0.25 - 0.35	1.5 max.	< 10	1.5 max.	< 10
13A	0.3 - 0.6	1.5 max.	< 10	2 max.	< 10
14	0.6 - 1.0	2 max.	< 10	2 max.	< 10
14A	0.6 - 1.2	1.5 max.	< 10	1.5 max.	< 10
15	1.3 - 1.7	2 max.	< 25	2 max.	< 20
15A	2 - 3	2.5 max.	< 10	2 - 3 max.	< 10
16	0.7 - 1.2	2 max.	< 15	2.5 max.	< 10
16A	1.0 - 1.3	2 max.	< 10	1.5 max.	< 10
17	0.2 - 0.4	1.0 - 1.5	< 10	1 - 1.5	< 10
17A	0.1 - 0.2	1.0 - 1.5	< 10	1 - 1.5	< 10
18	1.5 - 2.5	2 - 2.5	< 10	2	< 15
18A	2.0 - 3.0	2.5 - 3	<20	2 - 2.5	< 20
19	4.5 - 6.0	3 - 4	< 15	4 - 4.5	< 10
19A	4.0 - 5.0	3 - 4	< 20	3 - 4	<20
20	1.5 - 3.0	2 - 2.5	< 10	1.5 - 2	< 15
20A	1.0 - 2.5	2	< 15	1.5 - 2	< 10
21	2.0 - 3.0	2 - 2.5	< 10	2 - 2.5	< 10
21A	3.5 - 5.0	2.5 - 3.5	< 15	2.5 - 3	< 15
22	1.5 - 2.5	1.5 - 2	< 10	1.5 - 2	< 10
22A	1.0 - 2.5	1 - 2	< 20	1.5 - 2	<20

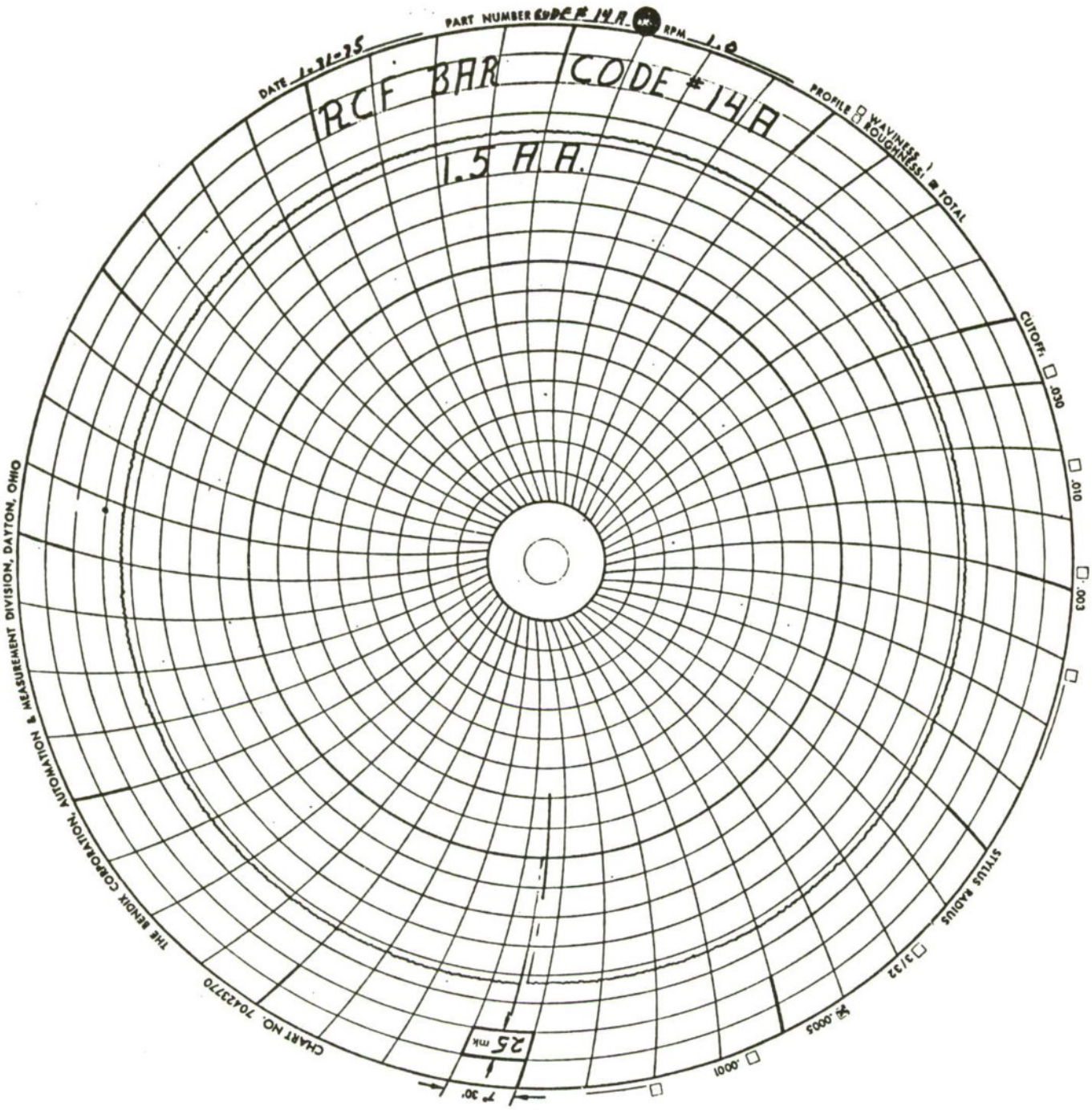

FIGURE 3 Excellent RCF rod roundness

specimen out-of-roundness was typically 1.3 microns (50 x 10^{-6} inches). The improved roundness may be attributed to higher grinding machine stiffness and the lower infeed during final grinding.

D. Rolling Contact Fatigue Test Equipment

The Rolling Contact Fatigue (RCF) test machine, developed by General Electric Company and marketed by Polymet Corporation, was used to measure specimen fatigue life at the Federal Mogul Research Laboratory. This machine has been used in previous RCF investigations[1,3,4] on silicon nitride and has been capable of differentiating between different methods of silicon nitride surface preparation and variations in material density.

The machine is shown in Figure 4. Two M-50 steel discs, 17.8 cm (7 in) in diameter and 1.27 cm (0.5 in) thick with a crown radius of 0.635 cm (0.25 in), are pressed against the rotating test specimen. The contact load is adjusted by means of a turnbuckle between the cantilever arms supporting the load discs and is measured with a strain gage. From the geometry of the contacting surfaces, the contact stresses for the non-lubricated contact can be calculated (see Appendix) for a given load. For example, for a load of 1.446 kN (325 lbs), the maximum compressive Hertz stress developed between a steel test specimen and steel loading discs is 4.83 MN/m^2 (700 ksi). The load necessary to produce this stress in a silicon nitride specimen with a steel disc is approximately 15 percent less because of the higher modulus of elasticity of the ceramic. For the silicon nitride-steel contact, a 1.446 kN (325 lbs) load produces a 5.52 MN/m^2 (800 ksi) compressive contact stress.

The RCF machine provides a rapid method for testing of bearing material under load in nearly pure rolling contact. The specimen is driven at 10,000 rpm and, since it receives two stress cycles per revolution, one hour produces 1.2 X 10^6 cycles. The fatigue life of a test is defined either by the number of cycles incurred before spall formation, which produces rig vibrations that cause automatic test termination, or by the number of cycles sustained before test suspension at an arbitrarily high number of cycles. The average test for M-50 steel, at 700 ksi Hertz stress, is about 2.5 X 10^6 cycles, or two hours. By comparison, an average "accelerated" full scale bearing test may run hundreds of hours.

The loading discs see the same maximum stress as the test specimen, but their relatively large diameter normally provides them a longer life than the specimens. However, they require refinishing when they spall, normally after 20-30 tests on steel, or when they flatten after extended use. The discs are requalified after refinishing and between silicon nitride tests, with a controlled group of M-50 steel specimens (Q-bars). The RCF test conditions used in the program are shown in Table X.

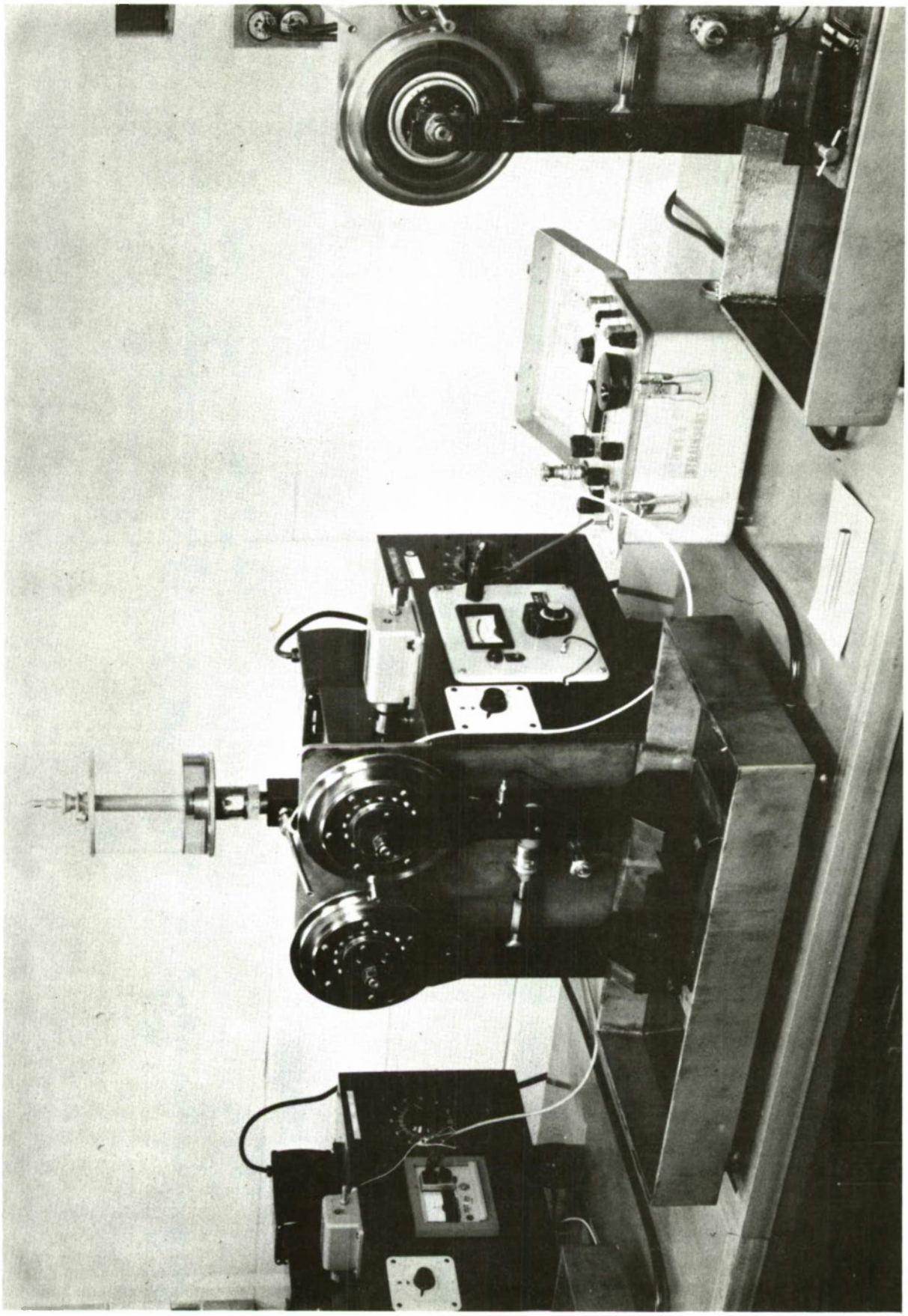

FIGURE 4 - Rolling contact fatigue test machines

TABLE X

RCF Test Conditions

Load - 1.45 Newtons (325 pounds)

Loading discs - M-50 steel

Compressive contact stress - Si_3N_4: 5.52 MN/m^2 (800 ksi)
M-50 Q bars: 4.83 MN/m^2 (700 ksi)

Speed - 10,000 rpm

Lubricant - Exxon 2380 Turbo Oil
Type II (MIL-L-23699B)

E. RCF Test Results

Early in the course of the RCF testing, it became apparent that the average silicon nitride fatigue life far exceeded silicon nitride lives previously encountered.[1,3,4] Lives in excess of 50 million stress cycles at 5.52 MN/m^2 (800 ksi) were common.

In addition, long fatigue tests were found to be self perpetuating as a result of load disc smoothing during test. This behavior was discovered by measuring fatigue lives on M-50 steel reference specimens during the use of the loading discs. Four pairs of load discs were involved in the study and each set was run against Q-bars before and after a long time silicon nitride suspended test. The fatigue comparisons are shown in Table XI.

TABLE XI

Effect of Si_3N_4 Test Life on Loading Discs

Disc Set	M-50 Life Before Si_3N_4 Test	Suspended Si_3N_4 Test Life	M-50 Life After Si_3N_4 Test	Circumferential Finish of Disc	
				Before	After
1	3.4	50.0	4.4	11-15 11.5-12.5	8-9 9-10.5
2	3.8	51.7	8.3		
3	2.6	63.8	16.7		
4	4.6	165.1	34.5		

Lives in 10^6 stress cycles
Roughness in microinches, AA.

The fatigue life of the steel specimens increases dramatically as the silicon nitride test is run for longer times above 50 million cycles. Roughness profiles of Disc Set #1 were taken before and after the testing on silicon nitride. Both discs exhibited similar behavior, as illustrated in Figures 5 and 6 for one of the pair. The smoothing effect is minimal circumferentially, but is quite apparent in the upper axial traces. The value of continuing silicon nitride fatigue testing beyond 50 million cycles is thus questionable.

As a result of the existance of the very long lives and the tendency for long tests to continue, it was necessary to restructure the RCF test strategy by decreasing the number of fatigue tests to failure. A minimum of three tests were run on each of the fifteen RCF finishes. A given test was run until failure or 50 million stress cycles, whichever came first. Most of these tests resulted in test suspensions at, or greater than, 50×10^6 stress cycles. During this testing a small number of very short fatigue lives began to occur. Because of the greater importance in actual service of short time fatigue lives, a second test series was conducted wherein specimens were run to failure or suspended at approximately 10 million cycles, whichever came first. The main purpose of this second test series was to investigate more fully the statistical frequency of the short lived failures. Altogether, a total of 96 tests were conducted. The individual test lives are listed in Table XII.

The test results are summarized in Table XIII with respect to fatigue life categories. The category boundaries are arbitrary, but serve to help visualize the failure distribution. The "medium" category is divided into the failures and those tests suspended at approximately 10 million cycles. The "long" category lists failures and suspensions over 50 million cycles. Weibull analysis is not applicable for populations with such small portions of failure. There were only thirty failures for fifteen variables.

V MICROSCOPY OF SURFACE FINISHES AND SPECIMENS AFTER FATIGUE TESTING

Scanning electron microscopy was used to characterize the surface appearance of the finishes. RCF specimen finishes are shown in Figures 7 through 16; in all cases the rod axis is horizontal.

Figure 7 is of Finish Variation #5, that of a 320 grit diamond wheel grind. The surface is furrowed and plastically deformed by the grinding scratches. With a single exception to be shown, a given finish on HS-110 material was indistinguishable from the same finish on NC-132 material, and, therefore, only one material finish is shown. Figure 8 shows Finish Variation #14 produced by the

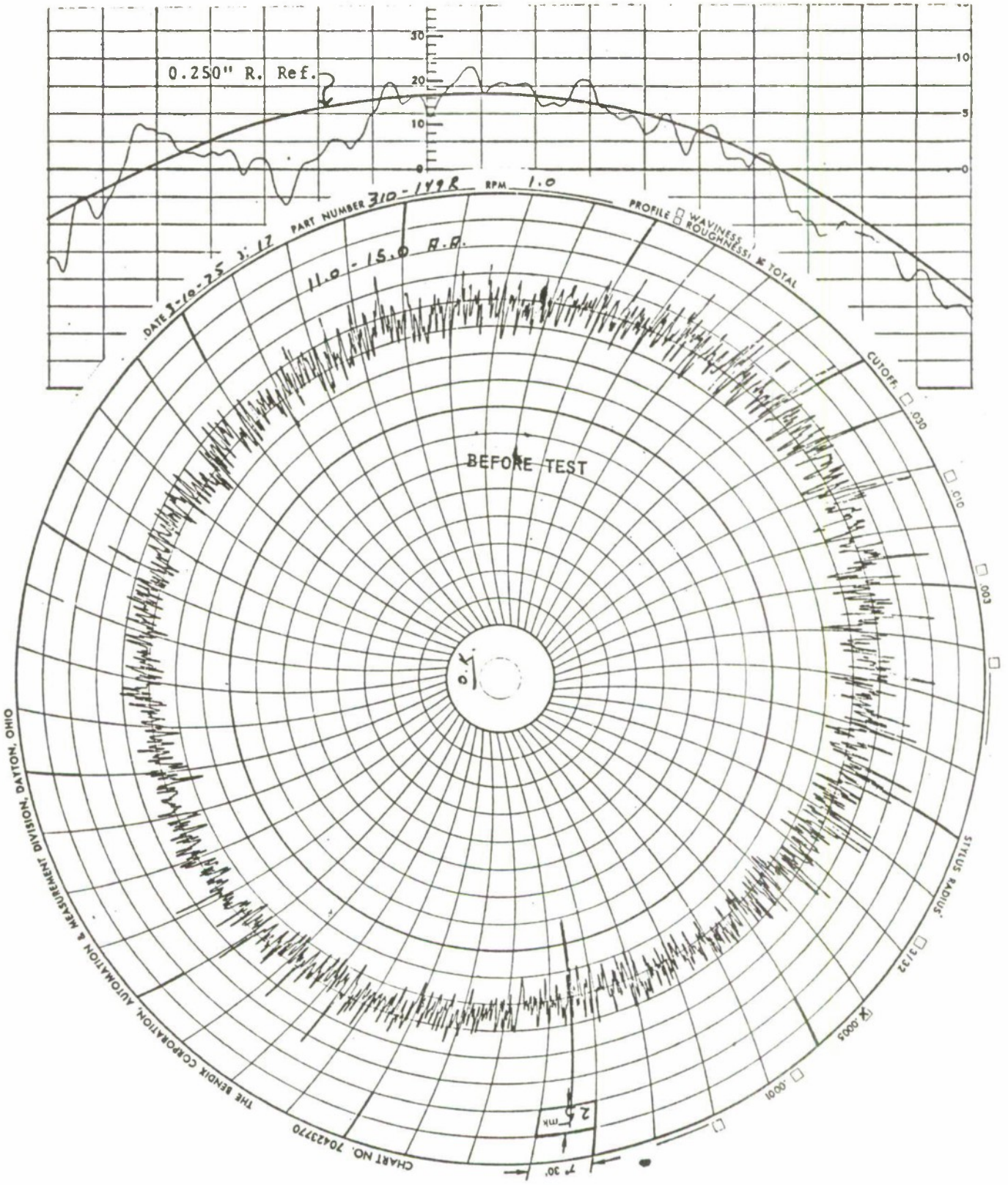

FIGURE 5 - Axial (top) and circumferential (bottom) profiles of load disc A, set 1 before silicon nitride test.

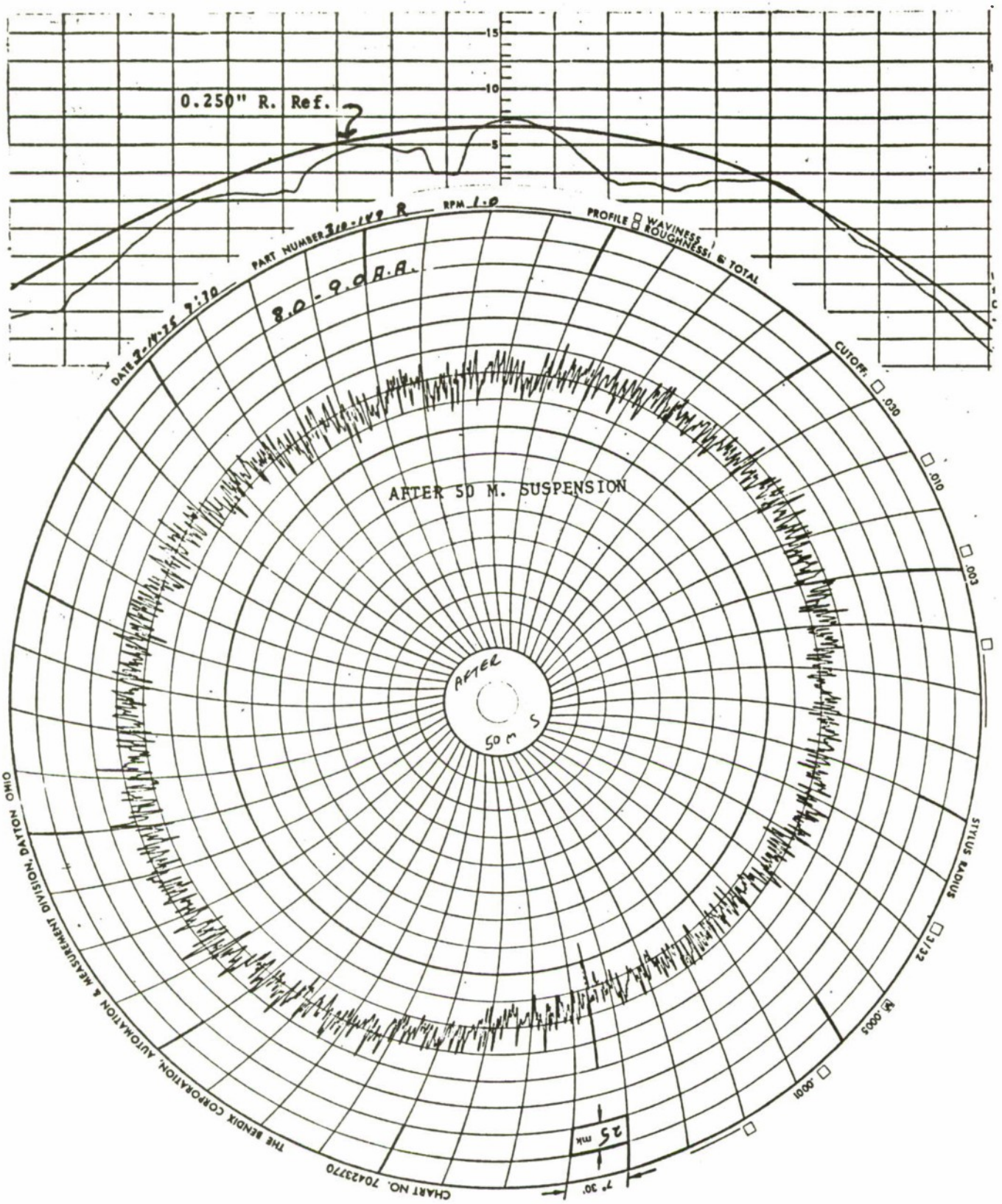

FIGURE 6 - Axial (top) and circumferential (bottom) profiles of load Disc A after 50 million cycles on silicon nitride

TABLE XII

Individual RCF test results

Si_3N_4 Type	Finish Variation	Rod Code #	Test #	Cycle Life	Test Termination
HS-110	5	8	1	138,029,000	S (=Suspension)
			2	50,007,000	S
			3	69,201,000	S
		8A	1	11,806,000	S
			2	9,695,000	S
			3	11,547,000	S
			4	11,236,000	S
			5	10,000,800	S
			6	9,729,200	S
			7	1,977,600	F (=Failure)
			8	1,250,600	F
HS-110	14	9	1	63,781,400	S
			2	80,632,000	F
			3	14,876,800	F
NC-132	5	10	1	165,096,400	S
			2	24,231,600	F
			3	5,546,800	F
NC-132	14	11	1	47,685,200	F
			2	76,331,800	F
		11A	1	79,117,600	S
HS-110	19	12	1	164,857,400	S
			2	58,704,400	S
			3	5,060,000	F
		12A	1	9,985,400	S
			2	6,489,000	F
			3	10,588,600	S
			4	9,024,600	S
			5	1,820,400	F
			6	11,732,000	S
			7	4,742,600	F
HS-110	23	13	1	51,688,000	S
			2	65,829,120	S
			3	26,185,800	F
NC-132	19	14	1	2,424,400	F
			2	7,593,600	F
		14A	1	5,253,600	F
			2	2,777,000	F
			3	11,032,000	S

TABLE XII (continued)

Si_3N_4 Type	Finish Variation	Rod Code #	Test #	Cycle Life	Test Termination
NC-132	20	15	1	90,691,600	S
			2	916,400	F
		15A	1	64,343,200	S
			2	9,464,400	S
			3	11,196,800	S
			4	11,671,800	S
			5	11,096,800	S
NC-132	21	16	1	117,899,000	S
			2	71,610,000	S
			3	10,835,740	F
		16A	1	10,578,800	S
			2	11,086,400	S
			3	12,378,800	S
			4	2,677,200	F
			5	673,400	F
			6	688,400	F
NC-132	22	17	1	30,258,000	F
			2	87,477,400	S
			3	615,400	F
		17A	1	2,844,800	F
			2	11,797,600	S
			3	11,191,200	S
			4	11,132,600	S
HS-110	17	18	1	59,258,000	S
			2	16,763,600	S
			3	93,010,000	F
			4	5,818,400	F
NC-132	15	19	1	77,184,400	S
			2	70,770,400	S
			3	33,668,000	S
			4	61,725,000	S
		19A	1	12,132,600	S
			2	9,687,400	S
			3	11,472,800	S
			4	11,290,440	S
			5	10,794,000	S
			6	11,647,200	S
			7	11,016,400	S
			8	10,038,200	S
			9	10,003,800	S
			10	11,372,800	S

TABLE XII (continued)

Si_3N_4 Type	Finish Variation	Rod Code #	Test #	Cycle Life	Test Termination
NC-132	17	20	1	120,310,600	S
			2	52,166,000	S
			3	50,524,800	S
		20A	1	11,070,200	S
			2	11,315,000	S
			3	10,620,800	S
			4	9,181,400	S
			5	11,094,000	S
			6	10,001,000	S
			7	11,467,800	S
			8	11,209,800	S
NC-132	26	21	1	55,269,400	S
			2	52,122,200	S
			3	20,614,820	F
NC-132	27	22	1	50,373,400	S
			2	39,748,400	F
			3	3,153,260	F

TABLE XIII

RCF Life (in 10^6 cycles) Summary by Life Category

Si_3N_4 Type	Finish Variation	Rod Finish Code #	'Very Short' 0.6-1.8	'Short' 2-4.9	'Medium' 5-49	'Medium' ~10 Suspension	'Long', ≥50 Failure	'Long', ≥50 Suspension
HS-110	5	8	1	1		6		3
HS-110	14	9			1		1	1
NC-132	5	10			2			1
NC-132	14	11			1		1	1
HS-110	19	12	1	1	2	4		2
HS-110	23	13			1			2
NC-132	19	14		2	2	1		
NC-132	20	15	1			4		2
NC-132	21	16	2	1	1	3		2
NC-132	22	17	1	1	1	3		1
HS-110	17	18			1	1	1	1
NC-132	15	19				11		3
NC-132	17	20				8		3
NC-132	26	21			1			2
NC-132	27	22		1	1			1
	Totals		6	7	14	41	3	25

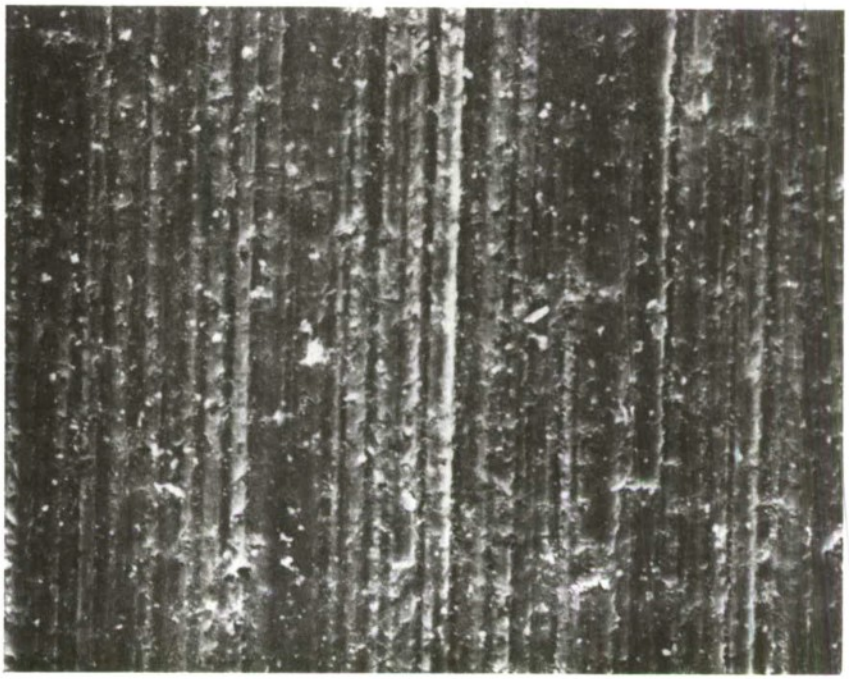

FIGURE 7 - Finish Variation #5 (320 grit diamond grind) on HS-110 Si_3N_4, 1000X.

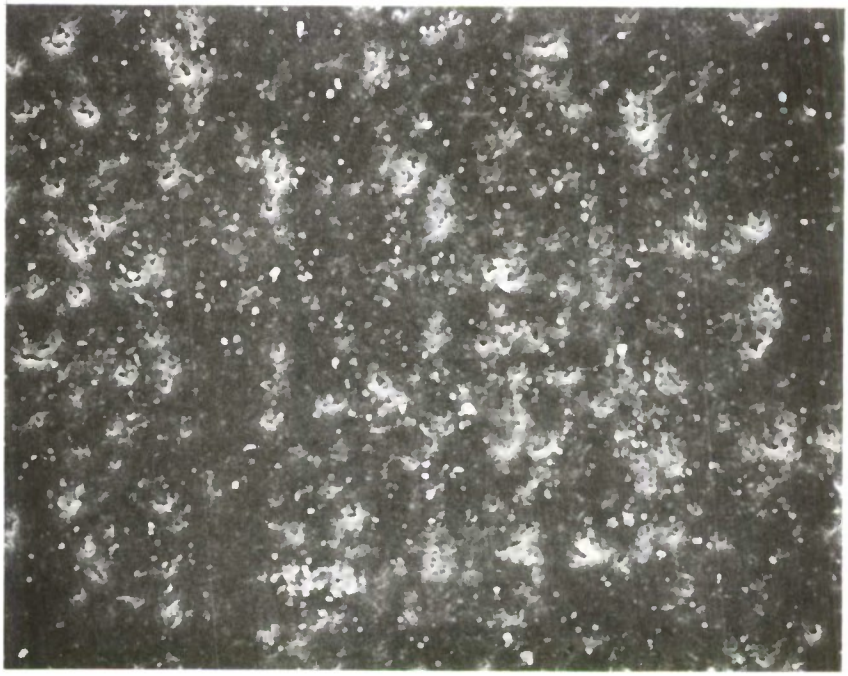

FIGURE 8 - Finish Variation #14 (150 grit SiC grind) on HS-110 Si_3N_4, 1000X.

150 grit silicon carbide wheel. Grinding furrows are absent due to the small grit penetration of the large worn grits. Considerable pitting is evident and which resulted from grain pull-out at regions of grain boundary damage. Figure 9 and 10 are of Finish Variation #19 (diamond paste lapping) on HS-110 and NC-132 silicon nitride, respectively. Microstructural details are apparent. The grains in the NC-132 silicon nitride show more background relief, while, in the HS-110, fine needle crystals ($\sim$ 2μ long) are present along with the more typical blocky crystals.

Figure 11 and 12 show finishing Variations #24 and #25 obtained by lapping with boron carbide and silicon carbide grits, respectively. The lack of sharp detail in both micrographs is believed due to the formation of a thin oxidation layer during lapping. The pits from grain pull-outs in Figure 12 appear to be filled with fine wear debris. The oxidation of the boron carbide abrasive is believed to contribute to the glass formation in Figure 11. The white specks in both micrographs are particles of tungsten carbide, which produce a greater yield of secondary electrons than the matrix. This is a typical appearance of NC-132 containing 2-4 percent WC.

Figure 13 and 14 show Finish Variations #22 and #23, obtained by polishing with SnO_2 and CeO, respectively. In both cases, the soft oxides have been packed into pull-outs, which contributes to the low surface roughnesses of these finishes. As in Figure 11, a residual loose abrasive scratch is visible in Figure 14.

Figure 15 shows Finish Variations #15 (400 grit diamond hone) while Figure 16 shows that of Finish Variation #17 (600 grit diamond hone). All honed finishes appeared basically similar; individual silicon nitride grains, substantial grain pull-out and traces of previous grinding scratches (vertical striations) are evident.

Figure 17 and 18 show two finishes which were applied to strength rods, but not to the RCF specimens. The former is of Finish Variation #24 (tumbling in B_4C grit after grinding). While the tumbling procedure did not remove the grinding scratch topography, impact pits were formed on the surface. Figure 18 shows the strong chemical attack of the hot fluorine etch (Variation #25).

As a result of the RCF test, the appearance of the surface within the circumferential load track changes. The extent of the altered appearance depends upon the original finishing procedure. The greatest change occurs in the diamond ground surfaces as shown in Figure 19 and which is to be compared with Figure 7. The severely disturbed material is removed as wear debris, leaving a pull-out pitted background and traces of the deepest grinding scratches. The degree of the amount of the intergranular fracture associated with pull-outs is believed to be related to the amount of sub-surface damage remaining after a given finishing operation.

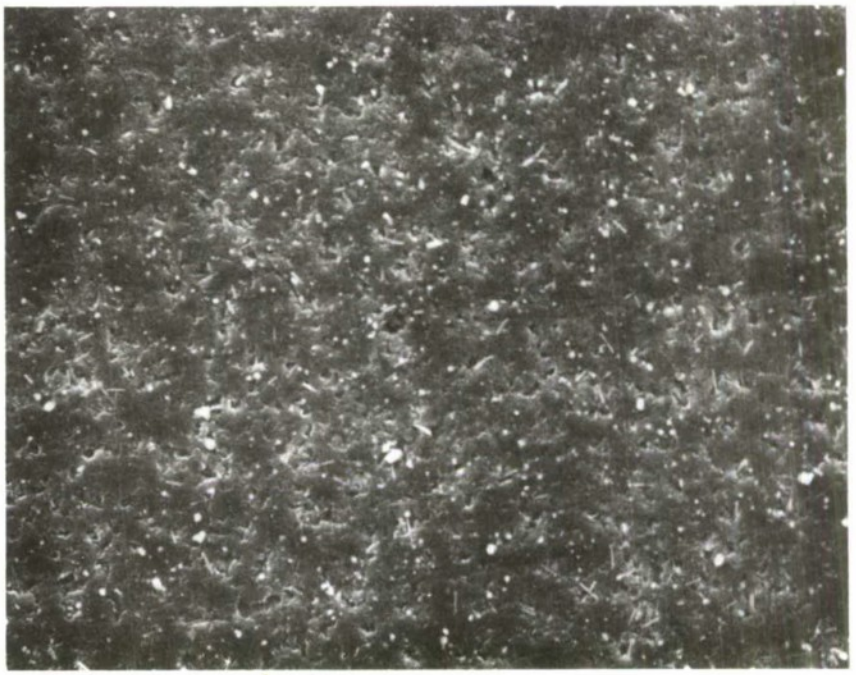

FIGURE 9 - Finish Variation #19 (diamond grit lap) on HS-110 Si_3N_4, 1000X.

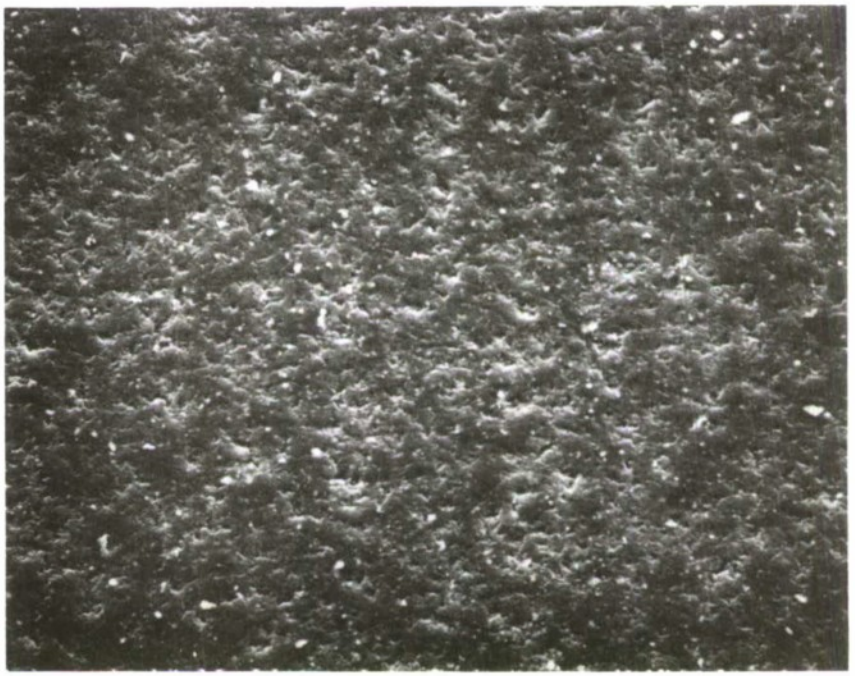

FIGURE 10 - Finish Variation #19 (diamond grit lap) on NC-132 Si_3N_4, 1000X.

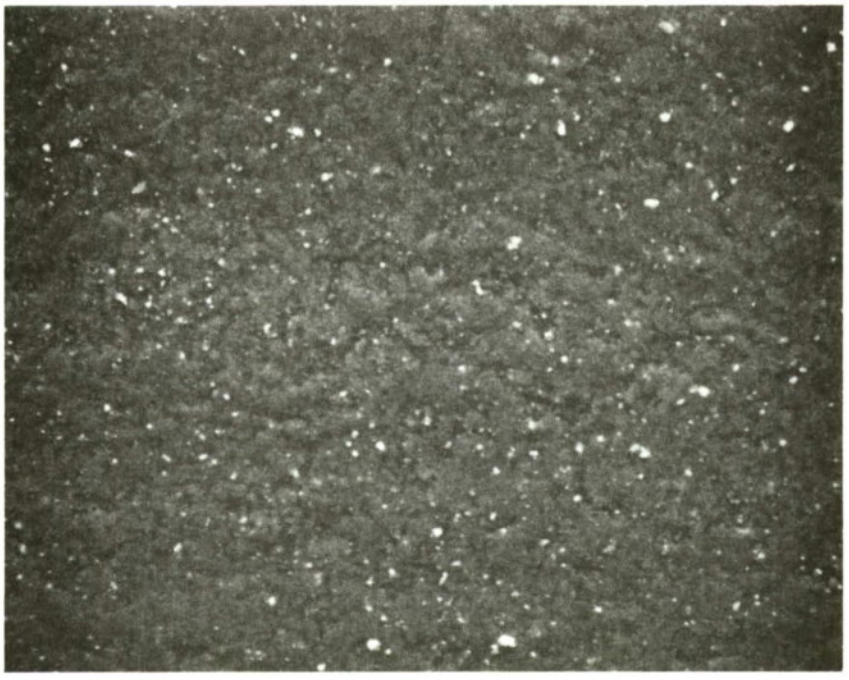

FIGURE 11 - Finish Variation #20 (B_4C grit lap) on NC-132 Si_3N_4, 1000X

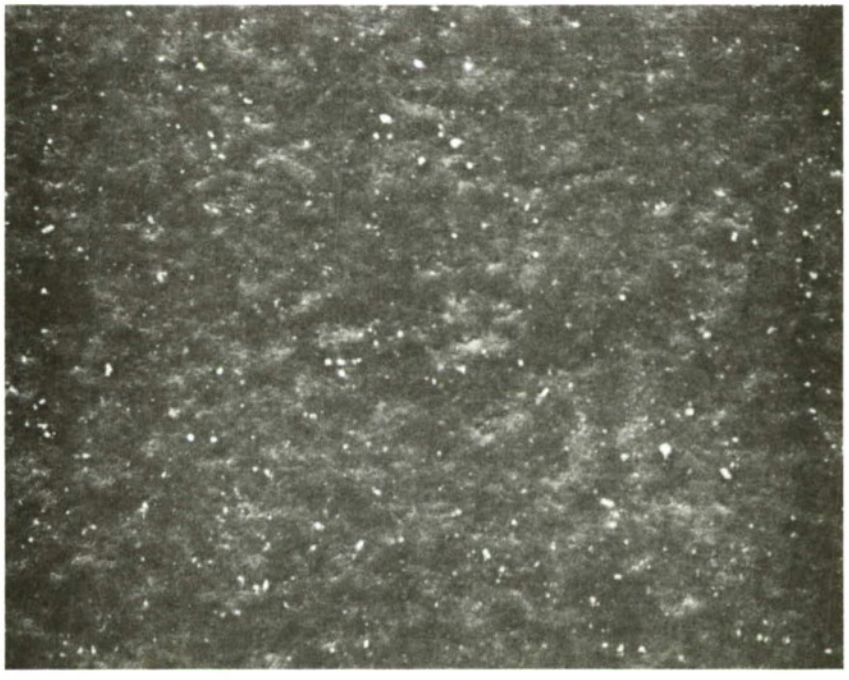

FIGURE 12 - Finish Variation #21 (SiC grit lap) on NC-132 Si_3N_4, 1000X.

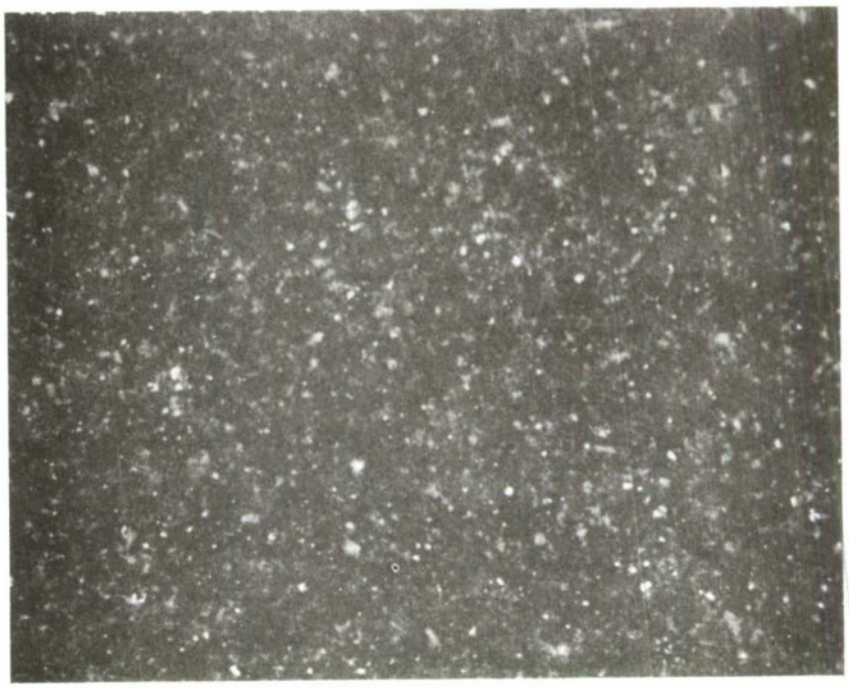

FIGURE 13 - Finish Variation #22 (SnO_2 polish lap) on NC-132 Si_3N_4, 1000X.

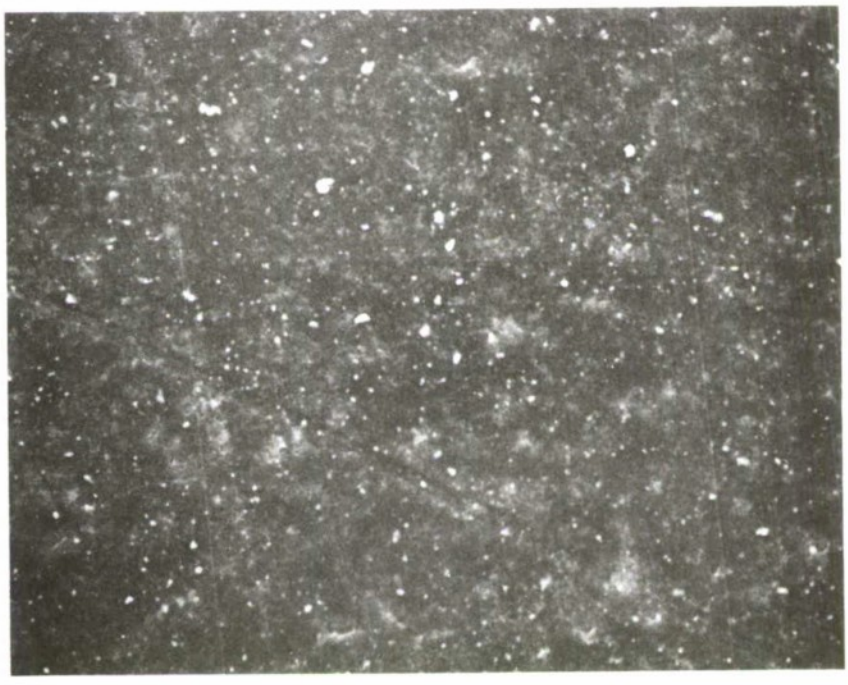

FIGURE 14 - Finish Variation #23 (CeO polish lap) on HS-110 Si_3N_4, 1000X.

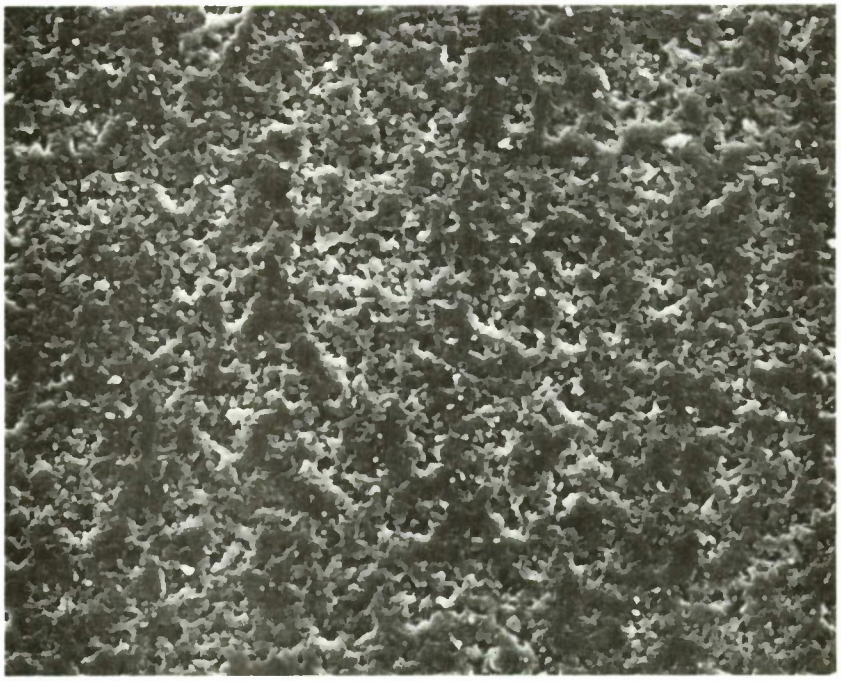

FIGURE 15 - Finish Variation #15 (400 grit hone) on NC-132 Si_3N_4, 1000X

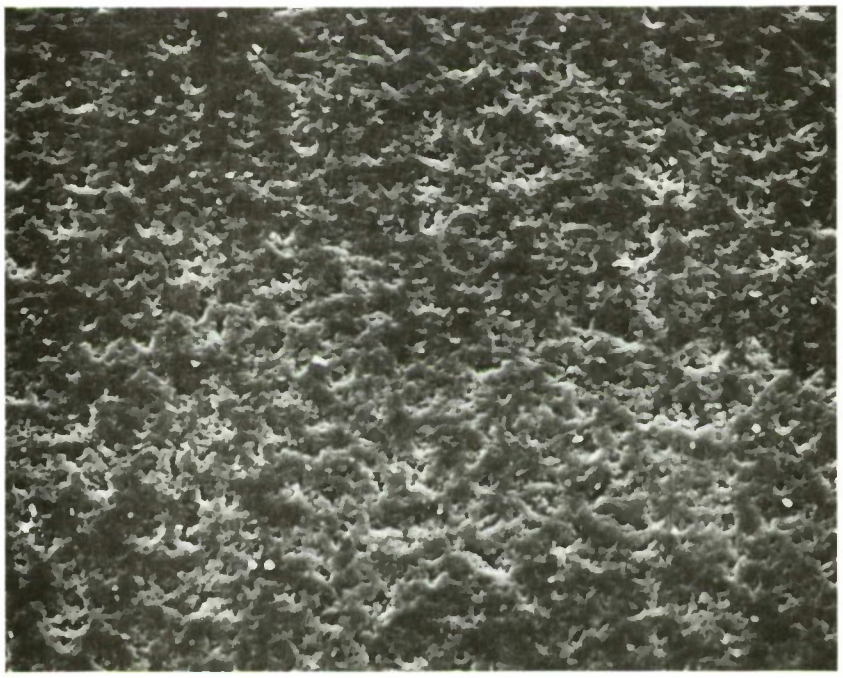

FIGURE 16 - Finish Variation #17 (600 grit hone) on NC-132 Si_3N_4, 1000X

FIGURE 17 - Finish Variation #24 (tumbling in B_4C grit after 320 grit diamond grind) on strength rod, 500X.

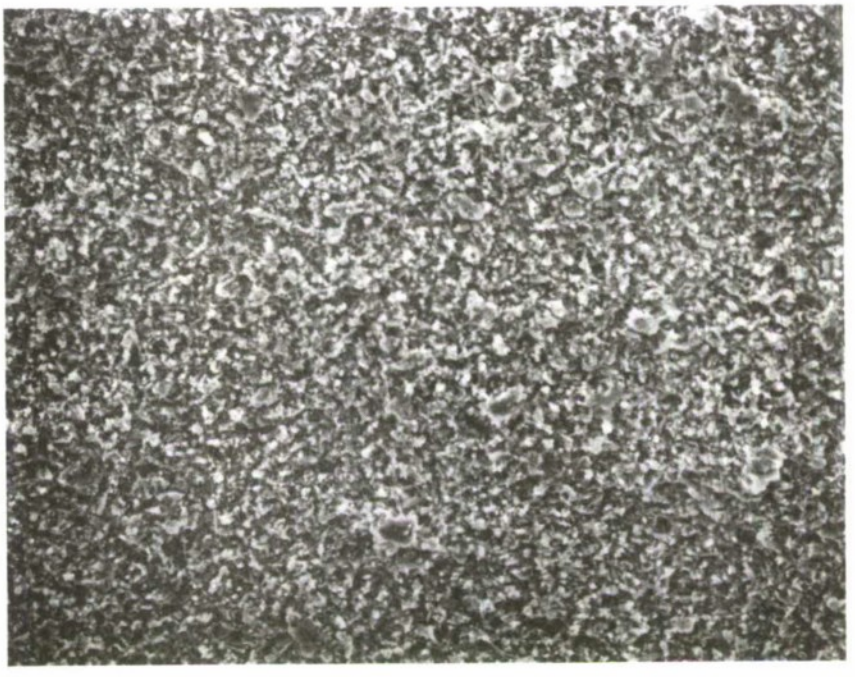

FIGURE 18 - Finish Variation #25 (gas etch) on strength rod, 500X.

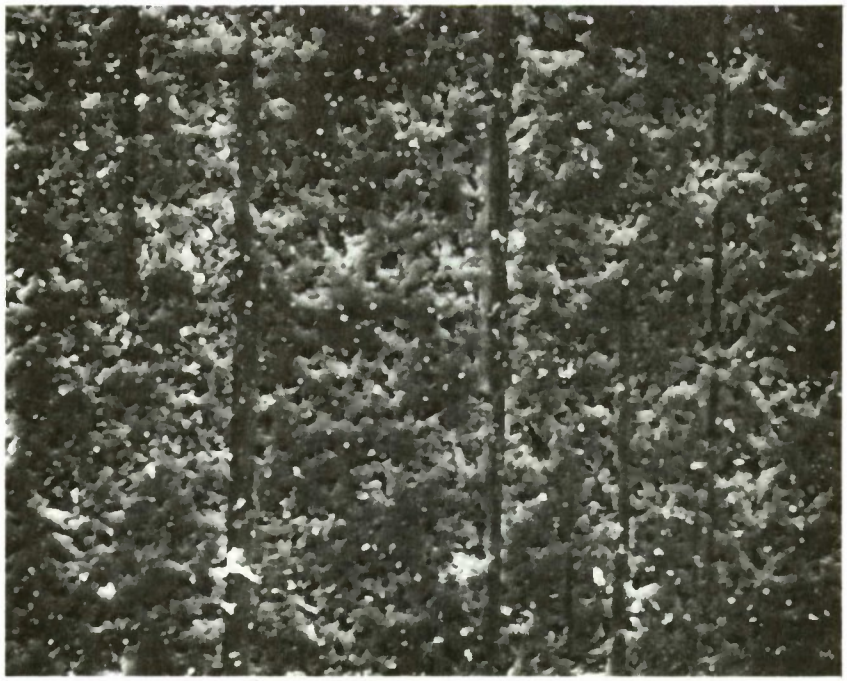

FIGURE 19 - Appearance of diamond ground surface after RCF test, 1000X.

Figure 20 shows that the impacted SnO_2 polishing compound is removed from the pull-outs within the load track. The appearance of the diamond lapped surface after RCF testing is relatively unchanged, as may be seen by comparing Figure 21 with Figure 10.

Typical examples of fatigue spalls formed on RCF specimens are shown in Figures 22 through 25. The load track is vertical and the specimen axis is horizontal in all photographs. As found in previous RCF testing on silicon nitride, the majority of spalls originate from a Hertz crack at the edge of the load track. The Hertz cracks border the contact zone around the circumference of the rod, although these cracks may be intermittent and only on one side of the contact zone. These cracks are analogous to cone cracks, which form when plates of brittle material are pressed with a spherical indentor, and arise from the large tensile contact stresses. However, in the RCF case, the cracks are not cones but slope down into the material on either side of the load track. Only infrequently do these cracks curl into the track.

The geometry of these contact stress cracks is drawn in Figure 26. The intersection of border cracks with the external surface

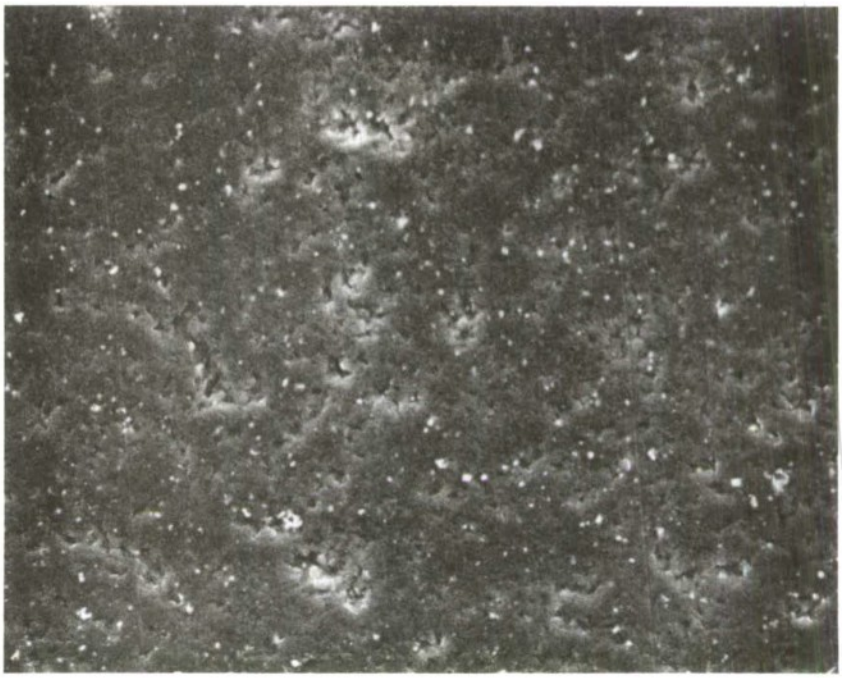

FIGURE 20 - Appearance of SnO_2 polished surface after RCF test, 1000X.

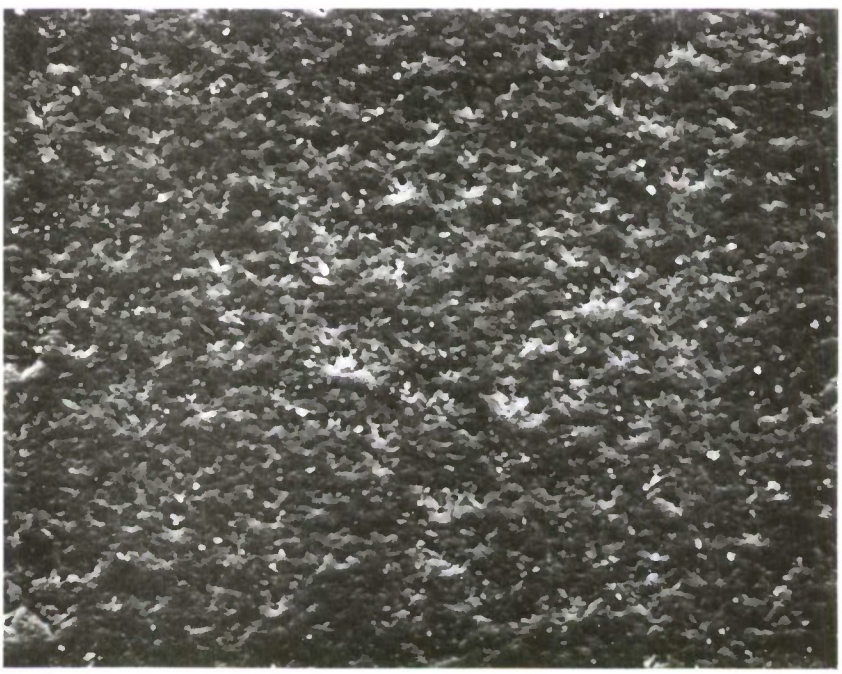

FIGURE 21 - Appearance of diamond grit lapped surface after RCF test, 1000X.

FIGURE 22 - Fatigue spall on RCF Rod #11 after 76.3 million cycles, 100X.

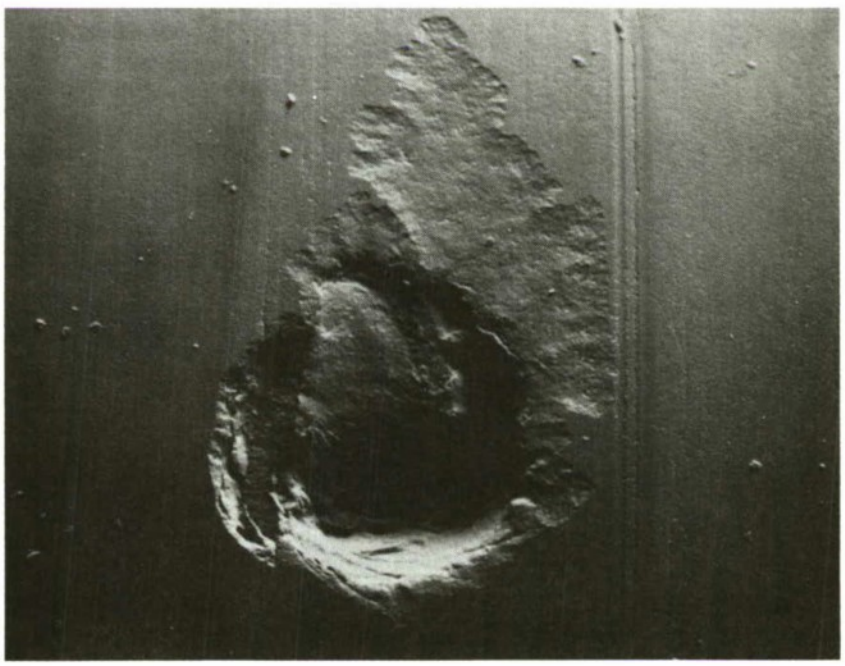

FIGURE 23 - Fatigue spall on RCF Rod #22 after 39.7 million cycles, 50X.

FIGURE 24 - Fatigue spall on RCF Rod #15 after 0.92 million cycles, 50X.

FIGURE 25 - Fatigue spall on RCF Rod #17 after 0.62 million cycles, 50X.

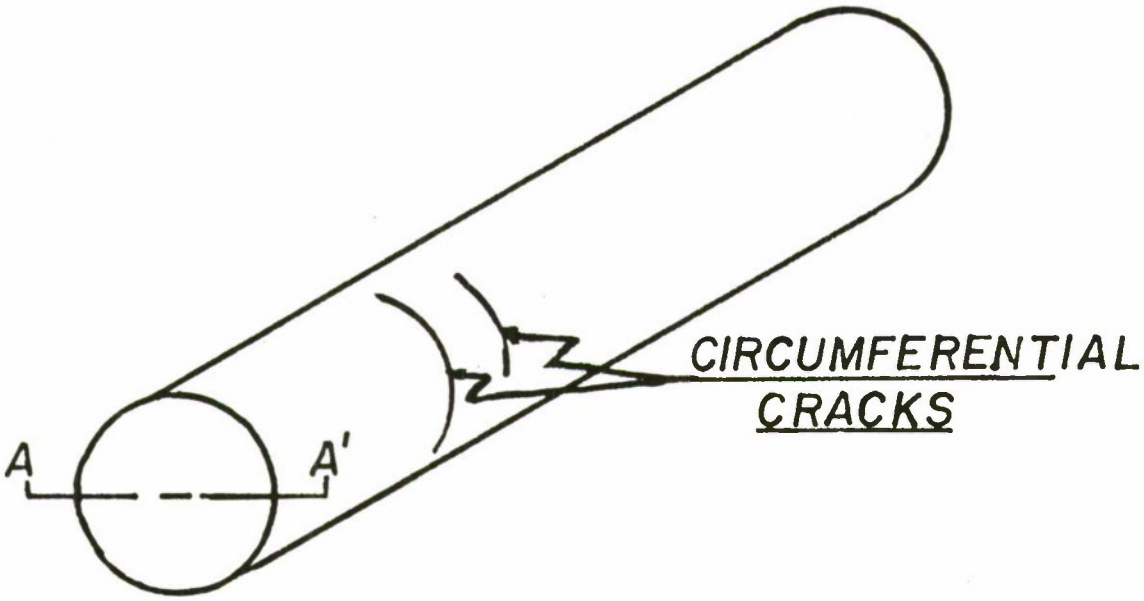

(A) SURFACE APPEARANCE OF CRACKS ON RCF ROD

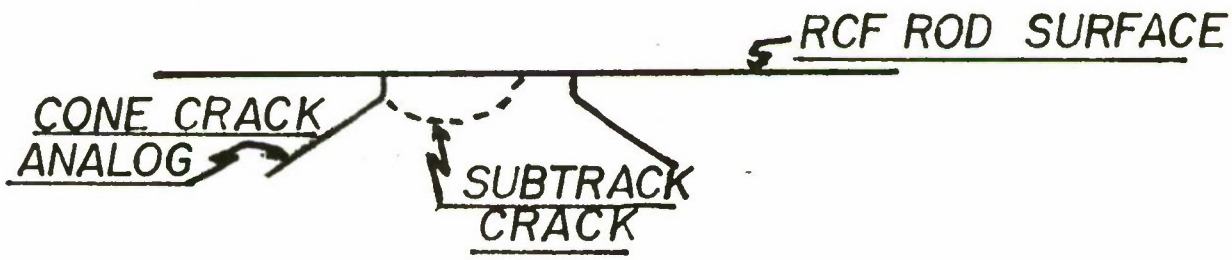

(B) AXIAL SECTION THROUGH A A'

FIGURE 26 **SCHEMATIC OF RCF ROD CRACKS**

is most clearly seen in the extreme right hand side of Figure 22. The contact stress cracks are true fatigue cracks in that numerous fatigue cycles are required for them to form. Subsequent to the border crack formation, a spall may form as the result of the propagation of a second crack beneath the contact zone. The origin of the second crack appears to be located at the point of slope change of the precedent cone crack analog.

The above spalling mechanism was responsible for most of the spalls. Of all the spalls, only three are believed to have initiated within the load track. There was no difference in spall appearance that could be attributed to material or finish type. Likewise, long lived spalls (Figures 22 and 23) were indistinguishable from short lived ones (Figures 24 and 25).

VI DISCUSSION

The silicon nitride rolling contact fatigue lives generated in this program are the longest ever experienced, both in terms of individual lives and frequency of occurrence, by the Norton-Federal Mogul researchers during their bearing work on silicon nitride at the 5.52 GN/m^2 (800 ksi) contact stress level.

This work resulted not only in a several times improvement in the overall fatigue life of silicon nitride in comparison with previous results, but also important differences in fatigue lives as a function of finishing procedures were uncovered. The understanding and application of these results to silicon nitride rolling element bearings should result not only in several times longer life than previously possible but in a reduced occurrence of short fatigue lives. This discussion is thus directed towards a clearer understanding of the critical elements responsible for these improvements.

A. Fatigue Life Ranking of Finishes

The extremely long lives prevented the occurrence of a sufficiently large number of fatigue test failures which would have enabled the application of Weibull statistics to determine an L_{10} life (time for 10 percent of the tests to produce failures) for a given surface finish. Although the absence of L_{10} values precludes a rigorous relative ranking of the finishes with respect to fatigue life, general life rankings can be drawn from the limited failure data.

Table XIV compares the fatigue lives of the two silicon nitride materials for those specimens with the same finishes. Neither material is obviously superior to the other; the relative higher percentage of HS-110 silicon nitride tests in the highest life category being offset by the greater incidence of very short failures.

TABLE XIV

HS-110 vs NC-132 Silicon Nitride Fatigue Life Comparison

Material	Finish Variation	Life Category (10^6 cycles) 'Very Short' 0.6-1.8	'Short' 2-4.9	'Medium' 5-49	'Medium' 10,Suspended	'Long' ≥50
HS-110	5	1	1	-	6	3
"	14	-	-	1	-	2
"	17	-	-	1	1	2
"	19	1	1	2	4	2
	Totals	2	2	4	11	9
NC-132	5	-	-	2	-	1
"	14	-	-	1	-	2
"	17	-	-	-	8	3
"	19	-	2	2	1	-
	Totals	0	2	5	9	6

Referring to Table XIII, on the basis of absence of very short failures and large predominance of long lives, Finishes #15 (400 grit hone) and #17 (600 grit hone after 320 grit diamond grind) give superior lives. Finishes #5 (320 grit diamond grind), #14 (150 grit SiC grind), #20 (B_4C lap), and #26 (600 grit hone after 150 grit diamond grind) appear to be above average. The worst performance was obtained on the NC-132 rods with Finish #19 (diamond lap), although the HS-110 rods with the same finish fared somewhat better. A more precise ranking of individual finishes would require additional testing failures.

Table XV compares the fatigue lives of the three major finishing methods of grinding, honing and lapping. Taken as a group, the lapped finishes have the poorest fatigue performance. The very short lives are strongly concentrated in the lapped finishes and they have a higher proportion of their lives in the 'short' and 'medium' categories than the other finishing methods. This is an unexpected result as the class of lapped finishes were the most geometrically perfect from the standpoint of both roundness and smoothness.

TABLE XV

Fatigue Life Failure Frequency vs Finishing Method

Finishing Class	Life Category (10^6 cycles) 'Very Short' 0.6 - 1.8	'Short' 2 - 4.9	'Medium' 5 - 49	'Long' >50
Grinding (Variations #5, 14)	1	1	4	8
Lapping (Variations #19-23)	5	5	7	9
Honing (Variations #15, 17, 26, 27)	0	1	3	11

(Suspensions at $\sim 10 \times 10^6$ cycles not included but suspensions at $\sim 50 \times 10^6$ cycles are included)

Examination of the RCF specimen rods at a low magnification under nearly specularly reflected light revealed that the lapped finishes possessed fine surface scratches. The scratches were sufficiently small and infrequent not to seriously influence the average surface roughness, but of a sufficiently high density to ensure, with a high degree of probability, that they would intersect any test track. The scratches are believed to have been caused by contamination of the lapping compound by larger abrasive particles. Although scratches were found near spalls, it was not possible to ascertain whether a scratch initiated the spall. Examples of these scratches may be seen in Figures 11 and 14. The most severe scratches were found on the NC-132 silicon nitride diamond lapped rods. These particular rods also gave the poorest fatigue performance. As diamond lapping was the penultimate finishing step in the preparation of the SnO_2 and CeO abrasive lapped finishes, it is conceivable that it could also have affected the fatigue results of the latter finishes. Based upon the above observations and the belief that increased surface perfection leads to an improved fatigue life, it is tentatively concluded that damage associated with the scratches is responsible for the reduced fatigue performance. This conclusion must be regarded as tentative since fine scratches were also observed on honed specimens, which had a relatively better fatigue performance. Two possible reasons why the fatigue lives of the honed specimens were not as reduced as the lapped specimens are flaw orientation and severity. The lapping scratches tended to be parallel to the rod axis while the honing scratches were predominately circumferential. An oversized

abrasive grit caught in the clearance between a specimen being lapped and the lap wall is expected to have a greater contact pressure associated with it (and therefore a greater probability of introducing microcracking) than a grit in a spring loaded hone.

Table XV indicates that the ground finishes are essentially equal to the honed finishes with respect to fatigue performance. This is an unexpected result as the honed samples are expected to have a lower severity of surface damage and, therefore, to be stronger. The result is also difficult to explain. On one hand, it can be argued that the strength difference between honed and ground surfaces on the RCF rods should be even greater than that shown in Table V for the strength rods. This argument is based on the greater uniformity of stock removal by honing on the RCF specimens; the strength rods were ground slightly out of round, which prevented a uniform layer of honed stock removal, thereby leaving more residual grinding damage. On the other hand, the finish grinding of the RCF rods prior to the honing operation was more gentle as a result of the reduced radial infeed per pass, which results in a smaller grit depth of cut. This could conceivably reduce the depth of grinding microcracks and thereby reduce the spread between the honed and ground strengths.

Even if more extensive testing confirmed that ground and honed silicon nitride bearing components had similar fatigue lives, a finish smoother than that obtainable with the 320 grit diamond grind (10 μ-in. AA) would be preferable for actual bearings with silicon nitride rolling components and steel races. The justification for the cost of the additional finishing operation to produce the smoother finish would be to prevent wear and a reduced fatigue life of the steel component. A 10 μ-inch roughness ensures the existance of a boundary lubricated contact and more mating surface interaction than is desireable. Rough silicon nitride surfaces in a steel/silicon nitride contact have been found to be more detrimental to the steel than an equally rough steel/steel contact.[6] Reducing the roughness of the contact surfaces may permit complete separation of the bearing surfaces by an oil film (elastohydrodynamic or EHD lubrication).

Another factor which could conceivably influence the propagation of flaws, but which is beyond the scope of this work, is the residual stress state of the surface of a given finish. Tensile stresses would facilitate, and compressive stress hinder, crack movement. It is known that grinding of silicon nitride does generate dislocation activity in the near surface region.[4] Alumina, which has roughly the same hardness as silicon nitride and, therefore, approximately the same resistance to plastic flow, has also been found to possess grinding induced dislocations and a residual compressive stress.[11] In addition to the magnitude and sign of any residual stress, the ratio of flaw-to-stress depth would determine whether residual stress would have a significant effect upon crack movement.

B. Comparison with Other RCF Results

As previously mentioned, the fatigue lives encountered during the current research are the longest ever experienced in the Norton-Federal Mogul investigations on silicon nitride. While it was the intent of the program to improve silicon nitride finishing procedures for bearing component applications, and that goal was achieved, it would be desireable to a) identify which finishing step or steps was responsible for the effect and b) verify that the life improvement was truly finishing related and not to some other variable. A comparison with previous results is useful for these purposes. In addition to finishing procedures, consideration was given to a) testing variables, b) material quality, c) specimen geometric perfection and d) lubrication effectiveness as potential life influencing variables.

Testing Variables - Although others[6,12,13,14] have conducted rolling contact fatigue studies on silicon nitride, the use of different types of testing machines and finishing procedures, the latter being undefined in some cases, makes those studies unsuitable for the comparison. In one study,[15] RCF specimens previously tested at Federal Mogul were retested at a second laboratory on a similar fatigue machine with longer lived fatigue results. This discrepancy illustrates the need for minimizing all test method variables when comparing data from different studies. The most appropriate study for comparison with the current study is that recently completed by the authors for the Naval Air Systems Command (NASC).[4] A portion of the NASC work also studied the RCF behavior of NC-132 silicon nitride. As that work was conducted by the same personnel on the same equipment under identical test conditions just prior to and during the early stages of the current work, testing variables are minimized.

The fatigue data from the NASC study is listed in Table XVI. Only four of the seventeen tests exceeded 20 million stress cycles.

TABLE XVI

Summary of Fatigue Data of Previously Tested[4] NC-132 Si_3N_4 Material

Ranked Test #	Fatigue Life (10^6 cycles)	Ranked Test #	Fatigue Life (10^6 cycles)
1	1.66	10	13.0
2	2.09	11	13.2
3	2.62	12	15.2
4	5.72	13	18.8
5	6.88	14	28.7
6	8.48	15	45.9
7	9.57	16	55.5
8	10.8	17	100.0
9	10.9		suspension

Material Quality - Both studies involved NC-132 grade silicon nitride plus at least one other grade of silicon nitride. The NC-132 silicon nitride billet material in the NASC program had a 4-Point strength of 861 MN/m^2 (124.9 ±27.4 ksi, essentially identical to the 841 ±103 MN/m^2 (122 ±15 ksi) strength of the current material. As far as is known, the quality of the two NC-132 billets is likewise comparable. Since the HS-110 material of the current study likewise had a fatigue life far in excess of all the NASC tested silicon nitride materials, the possibility that the better results were caused by a random fluctuation in billet quality is considered untenable.

Specimen Geometry - As a group, the geometrical perfection of the current RCF specimens exceeded that of previous specimens. It appears self evident that severely out of round RCF specimens are undesireable for test purposes, one reason being the variation in maximum contact load as the eccentric rod rotates against the cantilevered load discs. As fatigue life is inversely proportional to a positive exponential power of the contact load, the life of a contact having a variable maximum load would be less than that of a contact with a constant maximum load with the same time averaged load value. The magnitude of the out of roundness on a silicon nitride specimen that is required to promote such a life shortening effect is unknown and could not be evaluated within the current program.

However, a comparison of the specimen geometries of the 320 grit diamond ground specimens used in the two programs indicates that out of roundness differences can not explain the magnitude of the life differences. It is seen from Table IX, that Finish Variation #5 (320 grit diamond grind) on the NC-132 rods coded 10 and 10A produced an out of roundness just under 50 millionths and an axial roughness range of 8-13 μ-in. AA. Finish Variation #5 produced the specimens with the most out of roundness and roughest surface of all the finishes. These values are to be compared with the 42-60 millionths out of roundness and 8-10 μ-in. AA roughness of the NC-132 specimens prepared under the NASC study by a similar finishing procedure. It is concluded that superior specimen concentricity did not produce the superior fatifue life.

Lubrication Effectiveness - The transition from a boundary to an elastohydrodynamically lubricated contact situation can potentially occur if the bearing surfaces are sufficiently smooth, thereby resulting in greatly increasing fatigue life. A change in type of lubrication mode can not be involked to explain the improved fatigue performance, as the ∿10 μ-in. roughness of the load discs maintained boundary type lubrication for all silicon nitride finishes, independent of their roughnesses.

Finishing Procedures - The generally excellent fatigue lives of the ground and honed RCF specimens of the current program would seem to suggest a common cause for this superiority, should the

finishing procedures be responsible for the longer lives. The finishing procedures for the current fatigue rods are given in Table VII and that for the NASC specimens are given in Table XVII. The differences in the work speed and diamond wheel specification (plated grit, N grade, 75 concentration vs. unplated grit, R grade, 100 concentration) between the two studies are considered to be minor. The most significant difference in the finishing procedures of the two sets of specimens appears to be the factor of 5-10 smaller infeed in the final finishing grinding of the current specimens.

TABLE XVII

NASC RCF Rod Machining Conditions

Wheel Speed	= 1675 SMPM
Work Speed	= 600 rpm
Traverse	= 0.0025 cm (0.001")/work revolution
Diamond Grinding Wheels:	ASD100-R75B69 (roughing to 0.025 cm (0.010") oversize) ASD320-N75B69 (finishing)
Radial Infeeds:	0.0038 cm (0.0015")/pass (finishing) 0.0025 cm (0.001")/pass (finishing) 0.0013 cm (0.0005")/pass "Last few passes")
Coolant:	Norton Wheelmate 203, 1:50 with water

It is therefore inferred that the depth of grinding damage was less in the smaller infeed case and this led to the improved fatigue life; however, this conclusion should be verified by further experimentation.

In conclusion, while the longer fatigue lives experienced in the current program are believed to be a true effect, independent of material or test procedures, the cause for the enhanced life is not entirely clear. Reduced residual grinding damage is suggested as the most probable reason for the improved fatigue life.

C. Fatigue Testing Equipment

Although developed for steel bearing testing, the current RCF testing machine has proven to be very useful in the past for indicating material or finishing deficiences with silicon nitride.

However, the current program indicates that the utility of the machine is time limited when testing silicon nitride under optimum conditions. The limitation arises because of a) inability to further accelerate the test, by increasing the contact load, without invalidating the test by causing deformation in the loading discs and b) the deterioration of the steel loading discs during very long term tests. For these reasons, a modified or new type of RCF test is needed for the better performing specimens.

VII CONCLUSIONS AND RECOMMENDATIONS

The fatigue life of silicon nitride can be strongly influenced by finishing procedures. The grinding and honing finishes of this program produced the longest fatigue lives ever experienced by the Norton - Federal Mogul investigators. The superior fatigue behavior relative to past performance may be due to a reduced infeed during final diamond finish grinding. Silicon nitride bearing component finishes produced by diamond grinding (320 grit) in the last finishing step, while of adequate fatigue life, are too rough to run against steel components in an actual bearing. Acceptably smooth bearing component finishes, with essentially equivalent excellent fatigue life, may be obtained by light grinding with silicon carbide wheels from slight oversized dimensions. This approach enables the production of crowned roller geometries by the use of formed silicon carbide wheels.

It is possible to apply exceedingly fine bearing finishes to silicon nitride by a variety of techniques. However, the smoothest finishes, produced by lapping procedures, did not, in general, produce the longest fatigue lives. As a group, lapped finishes were inferior to other finishes investigated. This ranking is not believed to be characteristic of the lapping process itself, but rather due to damage associated with contamination of the lapping compounds with a larger sized abrasive grit.

The existance of infrequent, but very short, fatigue lives is a matter of concern as it is the short lives which control the useful life of real bearings. However, the clustering of the short lives in the lapped finishes indicates that this problem is finish related which can be avoided by using a modified lapping procedure or alternate finishing methods.

On the basis of the current work, Finishing Variations #15 and #17 (Table VIII, which involve diamond grinding and honing, would be recommended for producing silicon nitride rollers with a straight roller geometry. The use of a formad silicon carbide wheel after initial diamond wheel grinding, similar to Finish Variation #14, is recommended for shaping crowned roller geometries.

A need exists for a method to characterize reliably finishing damage on completed silicon nitride bearing components. Unfortunately, because of the small size of the relevant defects, no adequate inspection procedure exists at this time. A need also exists for a more rapid method of evaluating the effectiveness of the better silicon nitride finishes.

The following recommendations for future work on the finishing of silicon nitride bearing components are made:

1. Develop alternate means of evaluating finishes.

2. Investigate the effects on fatigue life of depth of infeed and wheel speed during diamond machining.

3. Investigate potential effects of a residual stress state on the ground surfaces, possibly by annealing studies or removal of uniform layers by a suitable etchant. Attempt to introduce compressive surface layers.

4. Investigate cause of short fatigue life failures to determine whether they arise from finishing or material deficiencies by means of extensive surface characterization before and after fatigue failures or by introducing (e.g. by Knoop hardness indentations) controlled depth microcracks prior to fatigue testing.

APPENDIX I**

RCF Stress Calculations*

The maximum Hertz stress for the RCF contact geometry, under non-lubricated conditons, is given by:

$$\sigma = \frac{C_\sigma \, C_d \, P^{1/3}}{(L/M)^{2/3}}$$

where, σ = maximum Hertz stress in psi

P = load in pounds

$$L = \frac{1 - \gamma_1^2}{E_1} + \frac{1 - \gamma_2^2}{E_2}$$

where E_i and γ_i are the Young's modulus and Poisson's ratio, respectively, of the i-th body,

$$M = 1/D_1 + 1/D_1' + 1/D_2 + 1/D_2'$$

where D_i and D_i' are the two orthogonal diameters of curvature for the i-th body

C_σ and C_d = Geometric parameters determined from the diameters D_1, D_1', D_2, D_2'.

The parameters, C_σ and C_d, may be read from Figure A1.

Table AI compiles the loading required to achieve the various maximum Hertz stress levels used in the RCF testing. The following values were used in the calculations:

$E_{steel} = 30 \times 10^6$ psi

$E_{silicon\ nitride} = 45 \times 10^6$ psi

$\gamma_{steel} = 0.29$

$\gamma_{silicon\ nitride} = 0.25$

$D_1 = 7"$ = diameter of loading wheel

$D_1' = 0.5"$ = loading wheel crown diameter

$D_2 = 0.375"$ = RCF rod diameter

$1/D_2' = 0.0$ (infinite curvature along rod axis)

---

*Blackett, Charles, Unpublished Federal-Mogul Corporation Internal Report #8122, November 1962.

**Appendix reproduced from Appendix of Reference 3.

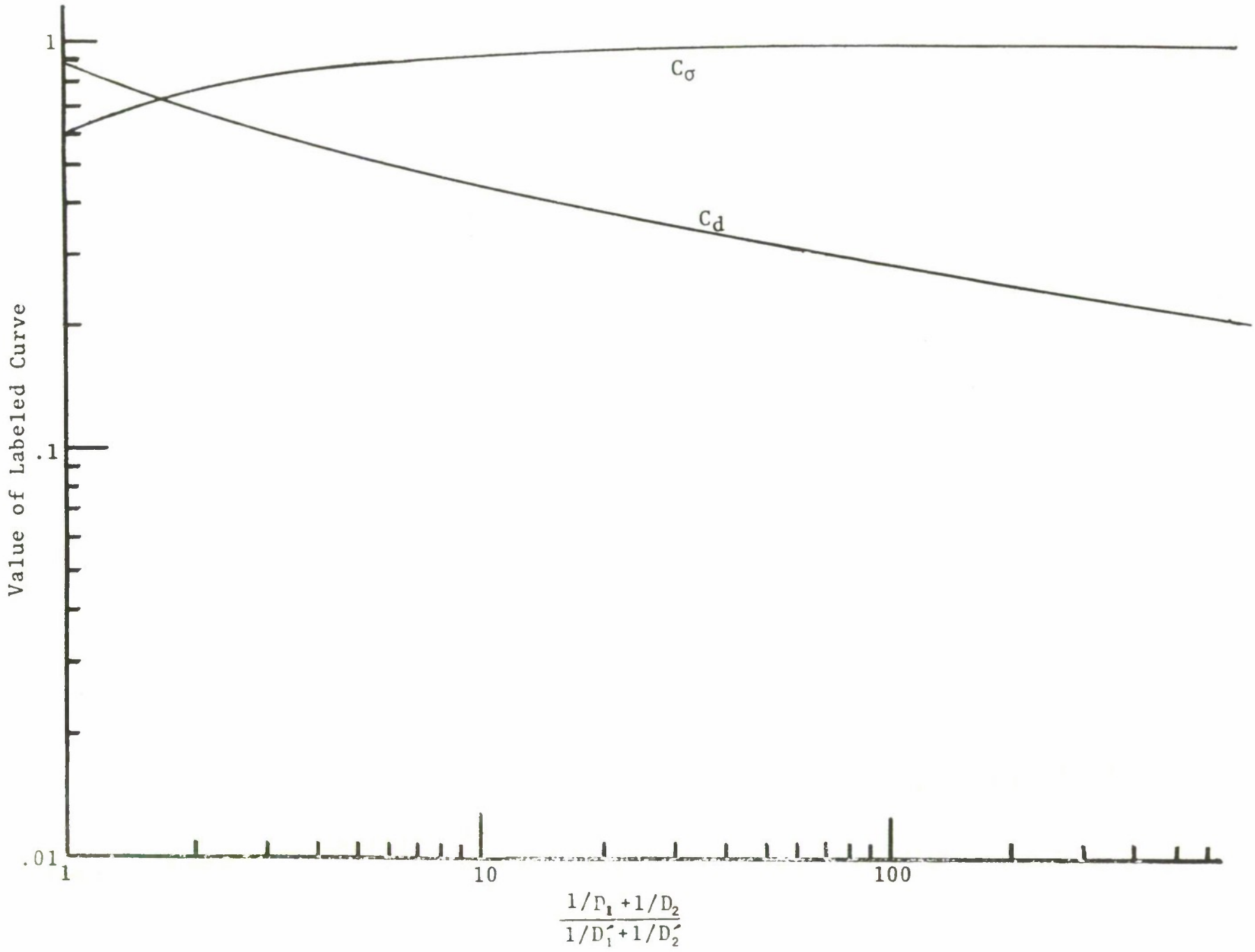
1
.1
.01
Value of Labeled Curve
C_σ
C_d
1
10
100
$\frac{1/D_1 + 1/D_2}{1/D_1' + 1/D_2'}$

TABLE AI

Bar Material	Disc Material	Pounds Load to Produce Specified Hertz Stress			
		600k	700k	750k	800k
M-50	M-50	205	325	-	-
Si_3N_4	M-50	140	220	275	325
Si_3N_4	Si_3N_4	89	140	-	210

REFERENCES

1. W. M. Wheildon, H. R. Baumgartner, D. V. Sundberg, M. L. Torti, Final Report on Contract N00019-72-C-0299, Feb. 1973.

2. H. R. Baumgartner and W. M. Wheildon, in Surfaces and Interfaces of Glass and Ceramics, V. B. Frechette, et.al. eds., Plenum Press, New York, 1973, p. 179.

3. H. R. Baumgartner, D. V. Sundberg and W. M. Wheildon, Final Report on Contract N00019-73-C-0193, Oct. 1973.

4. H. R. Baumgartner and P. E. Cowley, Final Report on Contract N00019-74-C-0157, August 1975.

5. R. R. Valori, L. B. Sibley and T. W. Tallian, Paper 65-Lubs-11, "Elastohydrodynamic Film Effects on the Load-Life Behavior of Rolling Contacts", presented at ASME Lubrication Symposium, June 6-9, 1965.

6. H. M. Dalal, Y. P. Chiu and E. Rabinowicz, ASLE Transactions, 18, (1975), 211.

7. W. A. Schmitt and J. E. Davey, NBS Special Pub. 348, May 1972, p. 259.

8. R. W. Rice, P. F. Becher, and W. A. Schmidt, ibid, p. 267.

9. F. I. Barotta, G. W. Driscoll and R. N. Katz, in Ceramics for High Performance Applications, J. J. Burke et. al. eds., Brook Hill Pub. Co., 1974, p. 445.

10. A. G. Evans and S. M. Wiederhorn, J. Mat. Sci., 9 (1974), 270.

11. B. J. Hockey, in NBS Special Pub. 348, May 1972, p. 333.

12. R. J. Parker and E. V. Zaretsky, NASA TMZ-68174 (1972).

13. R. J. Parker and E. V. Zaretsky, Paper No. 74-Lub-12, "Fatigue Life of High-Speed Ball Bearings with Silicon Nitride Balls" presented at ASME-ASLE Joint Conference, Montreal, Can., October 8-10, 1974.

14. J. M. Reddecliff, Final Report, NAPTC Contract N00140-75-C-0382, May 1975.

15. R. Valori, presented as NASC/ONR Program Review, held at King of Prussia, PA., Feb. 1974.

Army Materials and Mechanics Research Center,
Watertown, Massachusetts 02172
FINISHING TECHNIQUES FOR SILICON
NITRIDE BEARINGS -
H. R. Baumgartner - Norton Company
Paul E. Cowley - Federal Mogul Corporation

Technical Note AMMRC CTR 76-5, March 1976, 71 pp -
illus and tables, D/A Project: 7745506,
AMCMS Code 5397-07-5506

UNCLASSIFIED

Key Words

Silicon nitride
Bearings
Surface finishing
Physical properties
Characterization

Strength, surface finish and rolling contact fatigue life were determined on two grades of hot pressed silicon nitride after a total of twenty-seven different surface finishing procedures. Rollang contact fatigue lives of silicon nitride with selected smoother finishes tested at 800 ksi Hertz stress were an order of magnitude longer than those obtained on the M50 bearing steel controls and more than twice as long as the best results previously obtained on silicon nitride.

Army Materials and Mechanics Research Center,
Watertown, Massachusetts 02172
FINISHING TECHNIQUES FOR SILICON
NITRIDE BEARINGS -
H. R. Baumgartner - Norton Company
Paul E. Cowley - Federal Mogul Corporation

Technical Note AMMRC CTR 76-5, March 1976, 71 pp -
illus and tables, D/A Project: 7745506,
AMCMS Code 5397-07-5506

UNCLASSIFIED

Key Words

Silicon nitride
Bearings
Surface finishing
Physical properties
Characterization

Strength, surface finish and rolling contact fatigue life were determined on two grades of hot pressed silicon nitride after a total of twenty-seven different surface finishing procedures. Rollang contact fatigue lives of silicon nitride with selected smoother finishes tested at 800 ksi Hertz stress were an order of magnitude longer than those obtained on the M50 bearing steel controls and more than twice as long as the best results previously obtained on silicon nitride.

Army Materials and Mechanics Research Center,
Watertown, Massachusetts 02172
FINISHING TECHNIQUES FOR SILICON
NITRIDE BEARINGS -
H. R. Baumgartner - Norton Company
Paul E. Cowley - Federal Mogul Corporation

Technical Note AMMRC CTR 76-5, March 1976, 71 pp -
illus and tables, D/A Project: 7745506,
AMCMS Code 5397-07-5506

UNCLASSIFIED

Key Words

Silicon nitride
Bearings
Surface finishing
Physical properties
Characterization

Strength, surface finish and rolling contact fatigue life were determined on two grades of hot pressed silicon nitride after a total of twenty-seven different surface finishing procedures. Rollang contact fatigue lives of silicon nitride with selected smoother finishes tested at 800 ksi Hertz stress were an order of magnitude longer than those obtained on the M50 bearing steel controls and more than twice as long as the best results previously obtained on silicon nitride.

Army Materials and Mechanics Research Center,
Watertown, Massachusetts 02172
FINISHING TECHNIQUES FOR SILICON
NITRIDE BEARINGS -
H. R. Baumgartner - Norton Company
Paul E. Cowley - Federal Mogul Corporation

Technical Note AMMRC CTR 76-5, March 1976, 71 pp -
illus and tables, D/A Project: 7745506,
AMCMS Code 5397-07-5506

UNCLASSIFIED

Key Words

Silicon nitride
Bearings
Surface finishing
Physical properties
Characterization

Strength, surface finish and rolling contact fatigue life were determined on two grades of hot pressed silicon nitride after a total of twenty-seven different surface finishing procedures. Rollang contact fatigue lives of silicon nitride with selected smoother finishes tested at 800 ksi Hertz stress were an order of magnitude longer than those obtained on the M50 bearing steel controls and more than twice as long as the best results previously ebtained on silicon nitride.

Army Materials and Mechanics Research Center,
Watertown, Massachusetts 02172
FINISHING TECHNIQUES FOR SILICON
NITRIDE BEARINGS -
H. R. Baumgartner - Norton Company
Paul E. Cowley - Federal Mogul Corporation

Technical Note AMMRC CTR 76-5, March 1976, 71 pp -
illus and tables, D/A Project: 7745506,
AMCMS Code 5397-07-5506

UNCLASSIFIED

Key Words

Silicon nitride
Bearings
Surface finishing
Physical properties
Characterization

Strength, surface finish and rolling contact fatigue life were determined on two grades of hot pressed silicon nitride after a total of twenty-seven different surface finishing procedures. Rollang contact fatigue lives of silicon nitride with selected smoother finishes tested at 800 ksi Hertz stress were an order of magnitude longer than those obtained on the M50 bearing steel controls and more than twice as long as the best results previously obtained on silicon nitride.

Army Materials and Mechanics Research Center,
Watertown, Massachusetts 02172
FINISHING TECHNIQUES FOR SILICON
NITRIDE BEARINGS -
H. R. Baumgartner - Norton Company
Paul E. Cowley - Federal Mogul Corporation

Technical Note AMMRC CTR 76-5, March 1976, 71 pp -
illus and tables, D/A Project: 7745506,
AMCMS Code 5397-07-5506

UNCLASSIFIED

Key Words

Silicon nitride
Bearings
Surface finishing
Physical properties
Characterization

Strength, surface finish and rolling contact fatigue life were determined on two grades of hot pressed silicon nitride after a total of twenty-seven different surface finishing procedures. Rollang contact fatigue lives of silicon nitride with selected smoother finishes tested at 800 ksi Hertz stress were an order of magnitude longer than those obtained on the M50 bearing steel controls and more than twice as long as the best results previously obtained on silicon nitride.

Army Materials and Mechanics Research Center,
Watertown, Massachusetts 02172
FINISHING TECHNIQUES FOR SILICON
NITRIDE BEARINGS -
H. R. Baumgartner - Norton Company
Paul E. Cowley - Federal Mogul Corporation

Technical Note AMMRC CTR 76-5, March 1976, 71 pp -
illus and tables, D/A Project: 7745506,
AMCMS Code 5397-07-5506

UNCLASSIFIED

Key Words

Silicon nitride
Bearings
Surface finishing
Physical properties
Characterization

Strength, surface finish and rolling contact fatigue life were determined on two grades of hot pressed silicon nitride after a total of twenty-seven different surface finishing procedures. Rollang contact fatigue lives of silicon nitride with selected smoother finishes tested at 800 ksi Hertz stress were an order of magnitude longer than those obtained on the M50 bearing steel controls and more than twice as long as the best results previously obtained on silicon nitride.

Army Materials and Mechanics Research Center,
Watertown, Massachusetts 02172
FINISHING TECHNIQUES FOR SILICON
NITRIDE BEARINGS -
H. R. Baumgartner - Norton Company
Paul E. Cowley - Federal Mogul Corporation

Technical Note AMMRC CTR 76-5, March 1976, 71 pp -
illus and tables, D/A Project: 7745506,
AMCMS Code 5397-07-5506

UNCLASSIFIED

Key Words

Silicon nitride
Bearings
Surface finishing
Physical properties
Characterization

Strength, surface finish and rolling contact fatigue life were determined on two grades of hot pressed silicon nitride after a total of twenty-seven different surface finishing procedures. Rollang contact fatigue lives of silicon nitride with selected smoother finishes tested at 800 ksi Hertz stress were an order of magnitude longer than those obtained on the M50 bearing steel controls and more than twice as long as the best results previously obtained on silicon nitride.

ARMY MATERIALS AND MECHANICS RESEARCH CENTER
WATERTOWN, MASSACHUSETTS 02172

TECHNICAL REPORT DISTRIBUTION

No. of Copies	To
	Office of the Director, Defense Research and Engineering, Room 3 D1085, The Pentagon, Washington, DC 20301
1	ATTN: Mr. R. M. Standahar
12	Commander, Defense Documentation Center, Cameron Station, Alexandria, Virginia 22314
	Advanced Research Projects Agency, 1400 Wilson Blvd., Arlington, Virginia, 22209
1	ATTN: Director
1	Dr. Stickley, Director of Materials Sciences
	Metals and Ceramics Information Center, Battelle Memorial Institute, 505 King Avenue, Columbus, Ohio 43201
2	ATTN: Mr. Daniel Maykuth
	Chief of Research and Development, Department of the Army, Washington, DC 20310
1	ATTN: Physical and Engineering Sciences Division
1	Dr. Bernard R. Stein
1	Dr. James I. Bryant, DARD-ARS-PM
	Commander, U.S. Army Materiel Command, 5001 Eisenhower Avenue, Alexandria, Virginia 22333
1	ATTN: AMCRD-DE, Development Division
1	AMCRD-RS, Research Division
1	AMCRD-RS, Scientific Deputy
1	AMCRD-TC
	Commander, U.S. Army Aviation Systems Command, P.O. Box 209, Main Office, St. Louis, Missouri 63166
1	ATTN: AMSAV-LEP, Mr. J.M. Thorp
1	AMSAV-ER, Dr. I. Peterson
1	R. Long, Deputy Director, RD&E
	Commander, U.S. Army Missile Command, Redstone Arsenal, Alabama 35809
1	ATTN: AMSMI-IE, Mr. J. E. Kirshtein
1	AMSMI-R, Mr. John L. McDaniel
1	AMSMI-RBLD, Redstone Scientific Information Center
1	Chief Scientist, Dr. W. W. Carter
1	Directorate of R&D
1	Dr. B. Steverding

No. of Copies	To
	Commander, U.S. Army Mobility Equipment Command, 4300 Goodfellow Boulevard, St. Louis, Missouri 63120
1	ATTN: AMSME-PLC, Mr. J. Murphy
	Commander, U.S. Army Tank-Automotive Command, Warren, Michigan 48090
1	ATTN: AMSMO-PPS, Mr. David Siegel
1	Mr. J. P. Jones
1	AMSTA-BSL
	Commander, U.S. Army Armament Command, Rock Island, Illinois 61201
2	ATTN: Technical Library
1	AMSAR-SC, Dr. C. M. Hudson
1	AMSAR-PPW-PB, Mr. Francis X. Walter
	Commander, Aberdeen Proving Ground, Maryland 21005
3	ATTN: Technical Library, Building 313
	Commander, U.S. Army Foreign Science and Technology Center, 220 7th Street, N.E., Charlottesville, Virginia 22901
1	ATTN: AMXST-SD3
	Frankford Arsenal, Philadelphia, Pennsylvania 19137
1	ATTN: Pitman-Dunn Institute of Research
	Commander, Picatinny Arsenal, Dover, New Jersey 07801
1	ATTN: Feltman Research Laboratories
	Commander, Rock Island Arsenal, Rock Island, Illinois 61201
1	ATTN: SWERI-RDL
	Director, Eustis Directorate, U.S. Army Air Mobility Research and Development Laboratory, Fort Eustis, Virginia 23604
1	ATTN: Mr. J. Robinson, SAVDL-EU-SS
1	J. White, Assistant Technical Director
	Commander, U.S. Army Ballistic Research Laboratories, Aberdeen Proving Ground, Maryland 21005
1	ATTN: Dr. D. Eichelberger
	Director, U.S. Army Materiel Systems Analysis Activities Aberdeen Proving Ground, Maryland 21005
1	ATTN: AMXSY-D
	Commander, U.S. Army Electronics Command, 225 South 18th Street, Philadelphia, Pennsylvania 19103
1	ATTN: AMSEL-PP/P/IED-2, Mr. Wesley Karg

No. of Copies	To
	Commander, U.S. Army Mobility Equipment Research and Development Center, Fort Belvoir, Virginia 22060
2	ATTN: Technical Documents Center, Building 315
2	Mr. E. York, Matls. Res. Lab. STS-FB-GM
1	Mr. W. McGovern, AMCPM-FM
	Commander, U.S. Army Production Equipment Agency, Manufacturing Technology Branch, Rock Island Arsenal, Illinois 61202
1	ATTN: AMXPE, Mr. Ralph Siegel
	Commander, U.S. Army Research and Engineering Directorate, Warren, Michigan 48090
1	ATTN: SMOTA-RCM.1, Mr. Edward Moritz
1	SMOTA-RCM.1, Mr. Donald Phelps
	Commander, Watervliet Arsenal, Watervliet, New York 12189
1	ATTN: SWEWV-R
1	Dr. Robert Weigle
1	Chief, Bureau of Naval Weapons, Department of the Navy, Room 2225, Munitions Building, Washington, DC
	Chief, Bureau of Ships, Department of the Navy, Washington, DC 20315
1	ATTN: Code 341
	Chief of Naval Research, Arlington, Virginia 22217
1	ATTN: Code 472
	Office, Director of Research and Development, Department of the Air Force, The Pentagon, Washington, DC 20330
1	ATTN: AFDRD-OR, LTC Horas C. Hamlin
1	Major Donald Sponberg
	Headquarters, Aeronautical Systems Division, 4950 TEST W/TZHM (DH 2-5 Mgr), Wright-Patterson Air Force Base, Ohio 45433
1	ATTN: AFML-MATB, Mr. George Glenn
2	AFML-LAE, E. Morrissey
1	AFML-LMD, D.M. Forney
1	AFML-LC
1	AFML-LLS, R. Ruh
	National Aeronautics and Space Administration, Washington, DC 25046 21000 Brookpark Road, Cleveland, Ohio 44135
1	ATTN: Mr. G. Mervin Ault, Assistant Chief, M&S Division
1	Dr. H.B. Probst, MS 49-1
	National Aeronautics and Space Administration, Washington, DC 25046
1	ATTN: AFSS-AD, Office of Scientific and Technical Information
1	Mr. B.G. Achhammer
1	Mr. G.C. Deutsch, Chief, Materials Research Program, Code RR-1

No. of Copies	To
	National Aeronautics and Space Administration, Marshall Space Flight Center, Huntsville, Alabama 35812
1	ATTN: S&E-ME-MM, Mr. W.A. Wilson, Building 4720
1	R-P&VE-M, R.J. Schwinghamer
	Albany Metallurgy Research Center, Albany, Oregon 97321
1	ATTN: Mr. R.R. Wells, Research Director
	Defense Materials Service, General Services Administration, Washington, DC 20405
1	ATTN: Mr. Clarence A. Fredell, Director, Technical R&D Staff
	Director, Army Materials and Mechanics Research Center, Watertown, Massachusetts 02172
2	ATTN: DRXMR-PL
1	DRXMR-PR
1	DRXMR-CT
1	DRXMR-XC
1	DRXMR-AP
1	DRXMR-M
28	DRXMR-EO, Mr. G. Harris
2	DRXMR-EO, Dr. R.N. Katz
1	Commanding Officer, U.S. Army Aviation Material Laboratories, Fort Eustis, Virginia 23604
1	Dr. Raymond Bisplinghoff, Deputy Administrator, National Science Foundation, 1800 G. Street, NW., Washington, DC 20550
1	Dr. A. Lovelace, Deputy Assistant Secretary (R&D), Office of Assistant Secretary of the Air Force (Research & Development), Room 4E973, Pentagon, Washington, DC 20330
	U.S. Army Air Mobility Research and Development Laboratory, Advanced Systems Research Office, Ames Research Center, Moffett Field, California 94035
1	ATTN: F. Immen
1	J. Wheatly
	Ford Motor Company, Turbine Research Department, 20000 Rotunda Drive, Dearborn, Michigan 48121
1	ATTN: Mr. A.F. McLean
	IIT Research Institute, 10 West 35 Street, Chicago, Illinois 60616
1	ATTN: Mr. S. Bortz, Ceramics Research
	Midwest Research Institute, 425 Volker Boulevard, Kansas City, Missouri 64110
1	ATTN: Mr. Gordon E. Gross, Head, Physics Station

No. of Copies	To
	United Aircraft Research Laboratories, East Hartford, Connecticut 06108
1	ATTN: Dr. Michael DeCrescenti
	Westinghouse Electric Corporation Research Laboratories, Pittsburgh, Pennsylvania 15235
1	ATTN: Dr. R.J. Bratton
	Lehigh University, Department of Metallurgical Engineering, Bethlehem, Pennsylvania
1	ATTN: Prof. Richard M. Spriggs, Assistant to the President and Professor
1	Prof. D.P.H. Hasselman
	Massachusetts Institute of Technology, Department of Metallurgy and Materials Science, Cambridge, Massachusetts 02139
1	ATTN: Prof. R.L. Coble
	State University of New York, College of Ceramics at Alfred University, Alfred, New York 14802
1	ATTN: Mr. Satyavan Shukla, Assistant Librarian
1	Dr. A.R.C. Westwood, RIAS Division of the Martin Company, Baltimore, Maryland
1	Dr. S. Wiederhorn, National Bureau of Standards, Gaithersburgh, Maryland 20760
1	Dr. P. Jorgensen, Stanford Research Institute, Menlo Park, California 94025
1	SKF Industries, Inc., Engineering & Research Center, 1100 1st Avenue, King of Prussia, PA 19406 ATTN: Harish Dalal
	Deposits & Composites, Inc., 1821 Michael Drive, Reston, VA 22090
1	ATTN: Mr. Richard E. Engdahl, President
	TRW Inc., 23555 Euclid Avenue, Cleveland, OH 44117
1	ATTN: Ms. Elizabeth Barrett, T/M 3417
	Airesearch Mfg. Co. of Arizona, 402 South 36th Street, Phoenix, AZ 85034
1	ATTN: Chief, Materials Engineering Department, Dept. 93-39M
	Monsanto Research Corp., Dayton Laboratory, 1515 Nicholas Road, Dayton, OH 45407
1	ATTN: Mr. Richard J. Janowiecki, Research Group Leader
	Office of Naval Research, Naval Research Laboratory--Code 471 Arlington, VA 22217
1	ATTN: Dr. Arthur Diness

No. of Copies	To
	Naval Air System Command, Dept. of the Navy, Washington, DC 20360
1	Mr. Charles Bersch
	Norton Company, 1 New Bond Street, Worcester, MA 01606
1	ATTN: Dr. H.R. Baumgartner
	Federal Mogul Corporation, Bearing Group Research, 3980 Research Park Drive, Ann Arbor, Michigan 48104
1	ATTN: Mr. P.E. Cowley
1	Mr. M. Allen Magid, Materials Marketing Engineer, Florida R&D Center Pratt & Whitney Aircraft, P.O. Box 2691, West Palm Beach, FL 33402
	Naval Research Laboratory, Washington, DC 20390
1	ATTN: Mr. R. Rice
	Energy Research and Development Administration, Division of Transportation, Highway Vehicles Systems Branch, 20 Massachusetts Avenue, NW, Washington, DC
1	ATTN: Mr. G. Thur
1	Mr. R. Schulz